Journal of Medicinal Chemistry

Article

Rigidity versus flexibility: is this an issue in #1 (sigma-1) receptor ligand affinity and activity?

Frauke Weber, Stefanie Brune, Frederik Börgel, Katharina Korpis, Carsten Lange, Patrick J Bednarski, ERIK LAURINI, Maurizio Fermeglia, Sabrina Pricl, Dirk Schepmann, and Bernhard Wünsch

J. Med. Chem., **Just Accepted Manuscript** • DOI: 10.1021/acs.jmedchem.6b00585 • Publication Date (Web): 09 May 2016

ACS Publications

Journal of Medicinal Chemistry is published by the American Chemical Society. 1155 Sixteenth Street N.W., Washington, DC 20036

Rigidity versus flexibility: is this an issue in σ_1 (sigma-1) receptor ligand affinity and activity?

Frauke Weber,[a] Stefanie Brune,[a] Frederik Börgel,[a] Katharina Korpis,[b] Carsten Lange,[b] Patrick J. Bednarski,[b] Erik Laurini,[c] Maurizio Fermeglia,[c] Sabrina Pricl,[c,d] Dirk Schepmann,[a] Bernhard Wünsch[a,e]*

[a] Institute of Pharmaceutical and Medicinal Chemistry, University of Münster, Corrensstr. 48, D-48149 Münster, Germany

Tel.: +49-251-83-33311; Fax: +49-251-83-32144;wuensch@uni-muenster.de

[b] Institute of Pharmacy, Department of Pharmaceutical and Medicinal Chemistry, University of Greifswald, Friedrich-Ludwig-Jahn-Straße 17, 17487 Greifswald, Germany

[c] Molecular Simulations Engineering (MOSE) Laboratory, Department of Engineering and Architecture (DEA), University of Trieste, Via Valerio 6, 34127 Trieste, Italy

[d] National Interuniversity Consortium for Material Science and Technology (INSTM), Research Unit MOSE-DEA, University of Trieste, Via Valerio 6, 32127 Trieste, Italy

[e] Cells-in-Motion Cluster of Excellence (EXC 1003 – CiM), University Münster, Germany

Abstract

A set of stereoisomeric 2,5-diazabicyclo[2.2.2]octanes **14** and **15** was prepared in a chiral-pool synthesis starting from (*S*)- or (*R*)-aspartate. The key step in the synthesis was a Dieckmann-analogous cyclization of (dioxopiperazinyl)acetates **8**, which involved trapping of the intermediate hemiketal anion with Me_3SiCl. The σ_1 affinity was tested using membrane preparations from animal (guinea pig) and human origin. The binding of bicyclic compounds was analyzed by molecular dynamics simulations based on a 3D homology model of the σ_1 receptor. The good correlation between K_i values observed in the σ_1 assays and calculated free binding energy, coupled with the identification of four crucial ligand/receptor interactions allowed the formulation of structure affinity relationships. In an *in vitro* antitumor assay with seven human tumor cell lines, the bicyclic compounds inhibited selectively the growth of the cell line A427, which is due to induction of apoptosis. In this assay, the compounds behave like the known σ_1 receptor antagonist haloperidol.

Keywords

σ_1 Ligands, conformational restriction, Dieckmann analogous cyclization, structure affinity relationships, tumor cell lines, cytotoxic activity, 3D homology model, molecular dynamics, docking, ligand-receptor interactions

Introduction

After some misclassification as opioid receptors, σ receptors have now been shown to represent a receptor class on their own. To date, two subtypes are known, termed σ_1 and σ_2 receptor. These subtypes can be differentiated by their molecular weight,

tissue distribution, and ligand binding profiles. A particular feature is the different interaction of σ receptor subtypes with dextrorotatory benzomorphans.[1,2]

After cloning the σ_1 receptor from various tissues of animal origin including guinea pig liver, mouse brain, rat brain and rat kidney,[3-6] the σ_1 receptor was also cloned from the human chorioncarcinoma cell line.[7] The identity of σ_1 receptors cloned from different species is around 93%. The σ_1 receptor protein encoded by the human gene consists of 223 amino acids and has a molecular weight of 25.3 kDa. A similarity of the σ_1 receptor protein with other mammalian proteins could not be found, but a 30% identity and 67% similarity with the yeast enzyme sterol $\Delta^{8/7}$-isomerase was detected.[8]

High density of the σ_1 receptor was found in the central nervous system, but also in peripheral tissues, e.g. heart,[9] kidney, and liver.[10] Moreover, the σ_1 receptor was identified in endocrine organs,[11] immune competent blood cells[12] and very importantly in proliferating tumor cells.[13] The σ_1 receptor is a membrane bound protein localized predominantly in the plasma membrane, the membrane of the endoplasmic reticulum associated with mitochondria (mitochondria associated membrane) and around the nucleus (perinuclear region of ER).[14,15] It has been reported that the σ_1 receptor functions as chaperone interacting with different neurotransmitter receptors and ion channels, but the exact signal transduction pathway has not been identified so far.[16,17]

The σ_1 receptor plays an important role in various neurological disorders, including depression, psychosis, Alzheimer's disease, and alcohol/drug dependence.[18]

Furthermore, the antinociceptive system can be modulated by σ_1 receptors, i.e. σ_1 receptor agonists such as (+)-pentazocine are able to potentiate the analgesic potential of opioid analgesics.[19] Moreover, selective σ_1 receptor antagonists, e.g. S1RA, are able to reduce neuropathic pain.[20,21]

In 1990 overexpression of σ receptors in brain tumors was reported.[22] Then, high σ_1 receptor expression in human breast cancer cell lines and later, in small cell lung and prostate cancer cell lines was shown by immunocytochemical, immunohistochemical, and real-time-PCR studies as well Western blotting with a σ_1 receptor specific antibody.[23,24] These experiments led to the conclusion that the expression of σ_1 receptors in various human tumor cell lines is significantly increased compared with the σ_1 receptor expression level of the corresponding non-tumor cells.[25,26] In addition to the high expression level of σ_1 receptors in human tumor cells, it was shown that they are involved in apoptosis (programmed cell death) and σ_1 receptor antagonists were able to induce caspase-dependent cell death.[27] Therefore, selective targeting of σ_1 receptors represents a promising strategy for the therapy of cancer either alone or as adjuvants in chemotherapy by inducing apoptosis and ultimately cell death. In fact, treatment of tumor cells with various σ_1 ligands, e.g. the σ_1 antagonist haloperidol, led to both cytostatic and cytotoxic effects, although the molecular mechanisms underlying cell growth inhibition have not yet been clarified.[24,28] In addition to blocking σ_1 receptors, activation of σ_2 receptors, which are highly expressed in rapidly proliferating tumor cells, also induced apoptotic processes.[26,28-31]

Substantial efforts have been spent in recent years in the design, synthesis and evaluation of potent and selective σ_1 ligands. Many of these well-established σ_1 ligands contain a piperazine ring.[32-35] Monocyclic piperazines **1** with a

conformationally flexible 3-hydroxypropyl side chain display moderate σ_1 affinity.[34] (Figure 1) Conformational restriction of flexible ligands is a general strategy in drug design to increase both binding affinity and selectivity for a particular target.[36] As a result of conformational restriction, the ligand loss of entropy during binding is reduced and, hence, its free binding energy is increased.

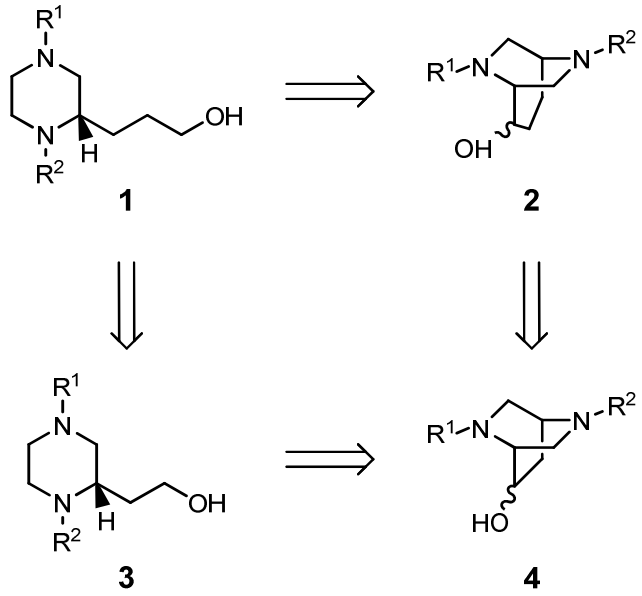

Figure 1: Development of ethano-bridged piperazines **4** from the ω-hydroxyalkyl substituted piperazines **1** and **3** and the propano-bridged piperazines **2**.

To investigate the influence of conformational restriction on σ_1 receptor affinity and cytotoxicity bridged piperazines **2** were designed by connecting the flexible 3-hydroxypropyl side chain of piperazines **1** with the piperazine ring. Receptor binding studies showed higher σ_1 affinity for the bridged piperazines **2** compared with the monocyclic piperazines **1**. For example, a K_i value of 188 nM was found for the flexible (hydroxypropyl)piperazine **1a** bearing *p*-methoxybenzyl (PMB) and benzyl (Bn) moieties (R^1 = PMB, R^2 = Bn) at the N-atoms.[34] After construction of the hydroxypropano bridge of **2** with appropriate configuration and the same substituents, the σ_1 affinity increased 30-fold (**2a** (R^1 = PMB, R^2 = Bn, (1*R*,2*R*,5*S*)-

configuration): K_i = 6.5 nM).[37] A similar relationship between the structure and the inhibition of tumor cell growth was observed: the cytotoxic effect against the human small cell lung cancer (SCLC) A427 cell line of the bridged piperazines **2** (e.g. **2a**: 54% inhibition at a concentration of 20 μM) was higher than the cytotoxic effect of the monocyclic piperazines **1** (e.g. **1a**: 23% inhibition at a concentration of 20 μM)[34,37] on the same cell line.

Recently we have shown that the σ_1 affinity of (2-hydroxyethyl)piperazines **3** was higher than that of their 3-hydroxypropyl homologs **1**, e.g. the (2-hydroxyethyl)piperazine **3a** (R^1 = PMB, R^2 = Bn, K_i = 20 nM) had a 9-fold higher σ_1 affinity than the (3-hydroxypropyl)piperazine **1a** (K_i = 188 nM) bearing the same substituents at the N-atoms.[34]

These observations prompted us to synthesize and evaluate the biological activity of the bicyclic compounds **4**, which are derived from the bicyclic compounds **2** by removal of one methylene moiety of the propano bridge, and from the 2-hydroxyethyl-substituted piperazines **3** by connecting the flexible hydroxyethyl side chain with the piperazine ring. On condition that conformational restriction should lead to higher σ_1 affinity and tumor cell growth inhibition, the designed 2,5-diazabicyclo[2.2.2]octanes **4** were expected to show improved biological activities. The results of this study were rationalized at the molecular level by atomistic molecular dynamics simulations of the interactions between ligands **4** and the recently developed 3D homology model of the σ_1 receptor.[38,39] These studies should lead to a deep understanding of the ligand - σ_1 receptor interactions and, moreover, the contribution of the particular structural elements to the overall interactions.

Synthesis

The synthesis of 2,5-diazabicyclo[2.2.2]octanes of type **4** was planned by bridging piperazinediones **8**-**10** with an appropriate side chain containing two carbon atoms. The dioxopiperazines **8a**-**d** with an acetate side chain were synthesized in a six-step reaction sequence starting from (*S*)-aspartate (**5**) as described in literature.[40] In brief, the diester **6**·HCl was reductively alkylated with different aldehydes and subsequently acylated to afford chloroacetamide **7**. The dioxopiperazines **8a**-**d** were obtained by a Domino reaction (S_N2 reaction followed by intramolecular aminolysis) of **7** with different primary amines. The differently substituted dioxopiperazines **8a**-**d** served as starting material for the exploration of different bridging strategies to obtain diazabicyclo[2.2.2]octanes (Scheme 1).

As demonstrated in preliminary investigations, the Dieckmann analogous cyclization of piperazinylacetates of type **8** provided less than 10% of the desired bicyclic products **12**. Therefore, alternative synthetic routes for the installation of the ethano bridge were investigated (reaction steps (h) and (i) in Scheme 1).

At first, aldehydes **11a**,**b** should be used as starting material, since the higher carbonyl activity of aldehydes **11** compared with esters **8** should give higher yields in the envisaged intramolecular aldol reaction. However, the direct reduction of the ester **8b** with DIBAL in toluene[41] did not lead to the aldehyde **11b**. Therefore, a two-step conversion of the ester **8b** into the aldehyde **11b** comprising a reduction and oxidation step was investigated. The selective reduction of the ester moiety of **8b** with $LiBH_4$ afforded the primary alcohol **10b** in 41% yield. However, subsequent oxidation of the primary alcohol **10b** with Dess-Martin periodinane[42] gave only very low yields of aldehyde **11b**. Finally, high yields of the aldehyde **11b** were obtained by

transformation of the ester **8b** into the Weinreb amide **9b**[43] and its subsequent reduction with $LiAlH_4$.

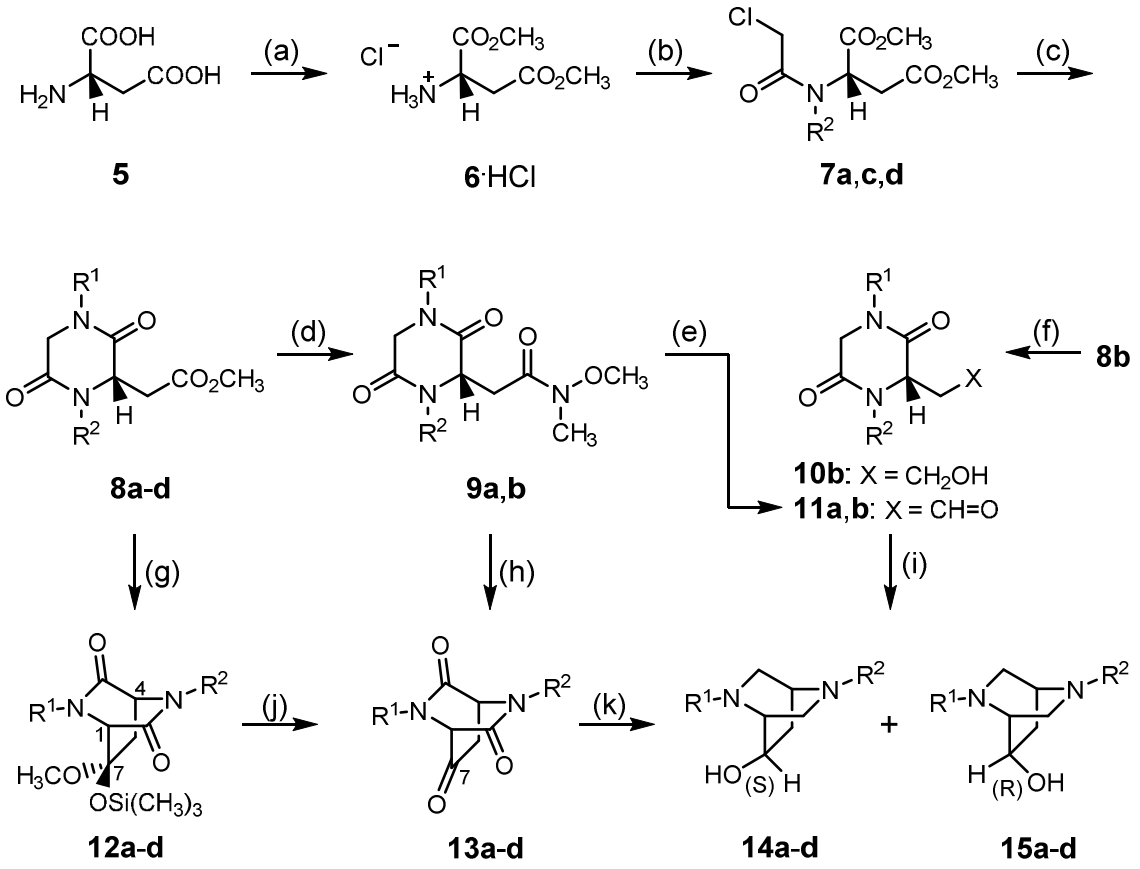

compounds **7**-**15**	R^1	R^2
a	$CH_2C_6H_{11}$	Bn
b	Me	Bn
c	$CH_2C_6H_{11}$	1-naphthylmethyl
d	$CH_2C_6H_{11}$	4-biphenylylmethyl

Scheme 1: Reagents and reaction conditions: (a) $(H_3C)_3SiCl$, H_3COH, rt, 16 h;[40] (b) 1. R^2-CH=O, NEt_3, CH_2Cl_2, rt, 16 h; 2. $NaBH_4$, H_3COH, 0 °C, 40 min; 3. $ClCH_2COCl$, NEt_3, CH_2Cl_2, rt, 2.5 h;[40] (c) R^1-NH_2, NEt_3, CH_3CN, rt, 16 h – 3 d;[40] (d) $HN(OCH_3)CH_3$·HCl, $Al(CH_3)_3$, CH_2Cl_2, rt, 5 h; (e) $LiAlH_4$, THF, -78 °C, 16 h; (f) $LiBH_4$, THF, -30 °C, 16 h;[21] (g) NaHMDS, THF, -78 °C, 40 min, then $(H_3C)_3SiCl$, -78 °C, 1 h, then rt, 2 h; (h) LiHMDS, THF, -78 °C, 16 h; (i) 1. LiHMDS, THF, -78 °C, 16 h; 2. $LiAlH_4$, THF, reflux, 16 h; (j) 0.5 M HCl, THF, rt, 16 h; (k) $LiAlH_4$, THF, reflux, 16 h.
The enantiomers of *ent*-**7** – *ent*-**15** were prepared in the same manner.

Reaction of the aldehyde **11b** with LiHMDS in THF at -78 °C induced the intramolecular aldol reaction affording a bicyclic product. Since the purification of the

cyclization product turned out to be difficult, the product was directly reduced with $LiAlH_4$ to provide the diastereomeric alcohols **14b** and **15b**. Although the ^1H NMR spectra showed the desired signals, the yields and the purity of the products were not sufficient for further investigations.

During the synthesis of the aldehyde **11a** the Weinreb amide **9a** had been synthesized. Weinreb amides can form stable chelates with metal cations after addition of nucleophiles.[44] Thus, after deprotonation of bislactam **9a** with LiHMDS at -78 °C, a stable Li^+-chelate was expected to form by intramolecular aldol reaction. Hydrolysis of the Li^+-chelate should then afford the bicyclic ketone **13a**. MS and NMR spectra confirmed the formation of **13a**. However, the yield of **13a** was below 5% and could not be increased although numerous variations of the reaction conditions (type and amount of base, temperature, reaction time) were investigated.

As a consequence of these results, the Dieckmann analogous cyclization[45] of esters **8** (conditions (g) in Scheme 1) was investigated in detail. For this purpose, the ester **8b** was treated with LiHMDS at -78 °C and the anion of the intermediate hemiketal was trapped after 10 min with $(CH_3)_3SiCl$ to obtain the mixed methyl silyl ketal **12b** in 3% yield. This variation of the Dieckmann condensation (trapping of the hemiketal anion) allows the formation of small bicyclic systems, which cannot form stabilized anions of β-dicarbonyl compounds at the end of the synthesis due to Bredt`s rule.[46,47] Herein, the first cyclization product (i.e. the anion of the hemiketal) was trapped by $(CH_3)_3SiCl$ after deprotonation of dioxopiperazine **8b** with LiHMDS. Due to the low yield of the mixed methyl silyl ketal **12b** with recovery of large amounts of the educt **8b**, this transformation was carefully optimized. In order to improve the yield of **12b**, different counter ions of the base and different time intervals for deprotonation and

trapping with $(CH_3)_3SiCl$ were evaluated. Systematic variations of the reaction conditions resulted in an improved yield of **12b** of 34%. In particular, the use of NaHMDS as base, an interval of 40 min for the deprotonation step, and a modified work up procedure (adsorption of the crude product on silica gel instead of dissolving the residue before purification by flash chromatography) represent the key features for achieving this yield. A previous X-ray crystal structure analysis[45] revealed that the Dieckmann analogous cyclization provided (7*R*)-configured products **12** with high diastereoselectivity. Since the transformation of all analogs provided predominantly one diastereomer with similar signals in the NMR spectra, the (7*R*)-configuration can be transferred to all mixed methyl silyl ketals **12**. The configuration of the chiral center in 4-position is defined by the configuration of the starting material (*S*)-aspartate (**5**) leading to (1*S*,4*S*,7*R*)-configuration of the mixed methyl silyl ketals **12**. Hydrolysis with 0.5 M HCl in THF led to the bicyclic ketone **13b**, which was reduced by $LiALH_4$ to yield the diastereomeric bicyclic alcohols **14b** and **15b**.

The same reaction sequence was used for the synthesis of **14a**,**c**,**d** and **15a**,**c**,**d** starting from esters **8a**,**c**,**d**. The reaction conditions for the crucial Dieckmann analogous cyclization of the esters **8a**,**c**,**d** had to be optimized for each compound individually. The yields were 26%, 13%, and 22% for **12a**, **12c** and **12d**, respectively.

In order to compare the σ_1 and σ_2 affinities of enantiomeric alcohols the (*R*)-configured dioxopiperazines *ent*-**8a**, *ent*-**8c** and *ent*-**8d** were prepared from (*R*)-aspartate (*ent*-**5**) and transformed into the bicyclic alcohols *ent*-**14a**, *ent*-**15a**, *ent*-**14c**, *ent*-**15c**, and *ent*-**14d**, *ent*-**15d**. Thus, all four possible stereoisomeric bicyclic alcohols with a cyclohexylmethyl residue at 2-position and different arylmethyl

residues at 5-position (series **a**, **c**, and **d**) were available for pharmacological evaluation.

In order to determine the enantiomeric purity a chiral HPLC method was developed to analyze the stereoisomeric benzyl substituted derivatives **14a**, *ent*-**14a**, **15a**, and *ent*-**15a**. Approximately 10 % of the enantiomers were found in the samples resulting from base catalyzed partial racemization during the bridging reaction of piperazinedione **8**. However, the contamination with small amounts of the enantiomer does not affect the biological activity of the compounds.

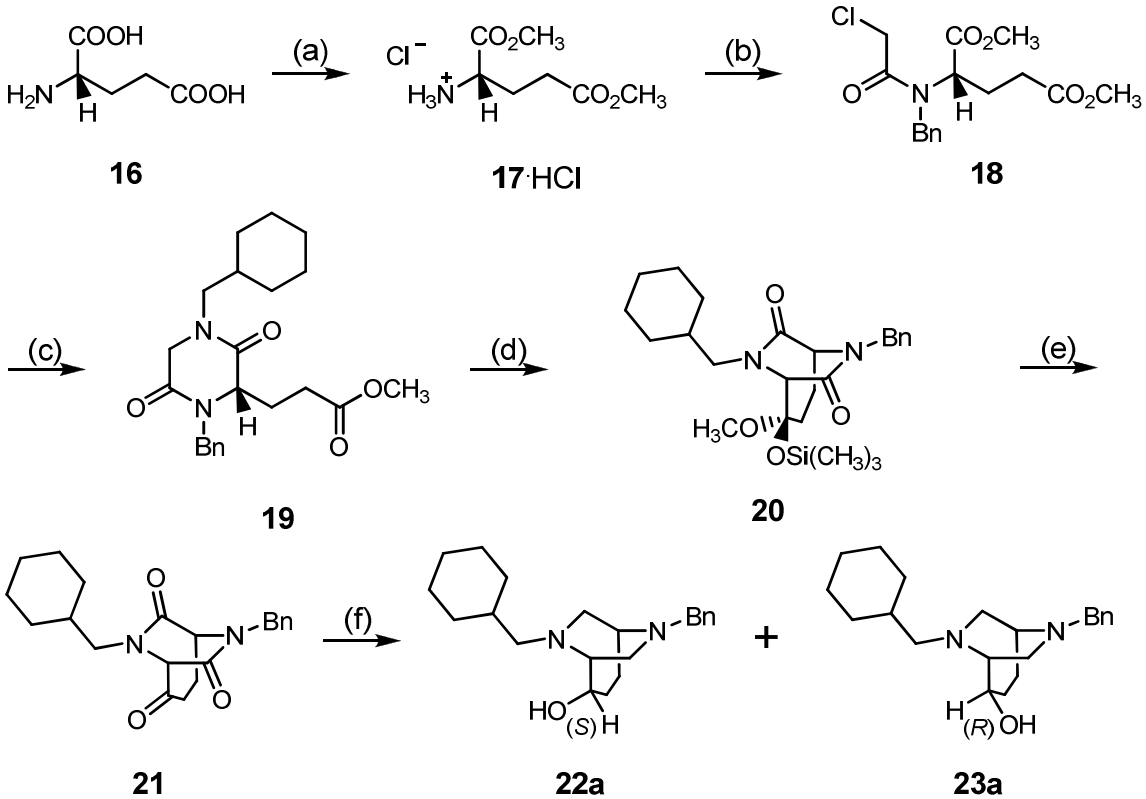

Scheme 2: Reagents and reaction conditions: (a) $(H_3C)_3SiCl$, H_3COH, rt, 16 h;[33] (b) 1. Ph-CH=O, NEt_3, CH_2Cl_2, rt, 16 h; 2. $NaBH_4$, H_3COH, 0 °C, 40 min; 3. $ClCH_2COCl$, NEt_3, CH_2Cl_2, rt, 2.5 h;[37] (c) $C_6H_{11}CH_2$-NH_2, NEt_3, CH_3CN, rt, 16 h; (d) NaHMDS, THF, -78 °C, 40 min, then $(H_3C)_3SiCl$, -78 °C, 1 h, then rt, 2 h; (e) 0.5 M HCl, THF, rt, 16 h; (f) $LiAlH_4$, THF, reflux, 16 h.

Since the pharmacological properties of the diazabicyclo[2.2.2]octanes **14**/**15** should be compared with those of the homologous diazabicyclo[3.2.2]nonanes, the diastereomeric alcohols **22a** and **23a** were prepared. (Scheme 2) Starting from (*S*)-glutamate (**16**) the dioxopiperazine **19** was obtained by esterification (**17**),[33] benzylation, chloroacetylation (**18**)[37] and, finally, cyclization with cyclohexylmethylamine. Deprotonation of **19** with NaHMDS at -78 °C and trapping of the intermediate hemiketal anion after 40 min with $(CH_3)_3SiCl$ provided the mixed methyl silyl ketal **20** in 60% yield. This result shows clearly that the moderate yields obtained during the cyclization of the smaller homologs **8** with an acetate side chain are due to the shorter bridge increasing the strain of the system. Hydrolysis of the mixed ketal **20** with diluted HCl led to the bicyclic ketone **21**, which was reduced with $LiAlH_4$ to obtain the diastereomeric alcohols **22a** and **23a** in 22% and 42% yields, respectively.

Pharmacological evaluation

Receptor binding studies

The σ affinities of compounds **14**/**15** and **22**/**23** were determined in competition experiments with the appropriate radioligands. All compounds were tested against σ_1 and σ_2 receptors of animal origin obtained from guinea pig (gp) brain (σ_1) and rat liver (σ_2), respectively. Additionally, the interaction of the ligands with human σ_1 receptors was analyzed using membrane preparations obtained from the peripheral blood human myeloma cell line RPMI 8226.[48] These experiments were performed to investigate the correlation between ligand interactions with human and guinea pig σ_1 receptors. [^{3}H]-(+)-Pentazocine served as radioligand for both σ_1 assays and [^{3}H]-DTG as radioligand in the σ_2 assay.[49-51] Compounds with high affinity were tested in

triplicate. For compounds with low σ affinity, only the inhibition of the radioligand binding at a test compound concentration of 1.0 μM is reported.

The results of the receptor binding studies of the new compounds are shown in Table 1. The σ_1 and σ_2 affinity data of various reference ligands are also listed for comparison. The values in Table 1 demonstrate that N-methyl substituted bridged piperazines **14b** and **15b** do not interact significantly with σ_1 and σ_2 receptors. This result correlates nicely with the low affinity observed for (hydroxyethyl)piperazines **3a**-**d** (Figure 1), which do not react with σ_1 and σ_2 receptors when R^1 is a small methyl residue (e.g. **3b**).

In the guinea pig assay the σ_1 affinity of bicyclic compounds **14** and **15** bearing a 2-cyclohexylmethyl substituent is generally in the low nanomolar range, only *ent*-**14a** and **15d** reveal K_i values higher than 20 nM. Whilst the stereoisomeric bicyclic 5-benzyl derivatives **14a**, **15a**, *ent*-**14a**, and *ent*-**15a** show similar σ_1 affinity as the corresponding (hydroxyethyl)piperazine **3a,** the σ_1 affinity of the bicyclic 5-naphthylmethyl (**c**-series, exception *ent*-**15c**) and biphenylylmethyl derivatives (**d**-series) display slightly reduced σ_1 affinity compared to their (hydroxyethyl)piperazine analogs **3c** and **3d**.

Table 1 σ_1 and σ_2 receptor affinity of bicyclic piperazines

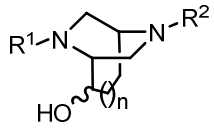

compd.	R^1	R^2	n	σ_1 (gp)[a] K_i ± SEM [nM]	σ_2 (rat)[b] K_i ± SEM [nM]	σ_1 (hum)[c] K_i ± SEM [nM]
3a[40]	$CH_2C_6H_{11}$	Bn	-	4.2 ± 1.1	116[e]	21 ± 4.0
3b[40]	CH_3	Bn	-	28%[d]	27%[d]	n.d.
3c[40]	$CH_2C_6H_{11}$	1-Naph-CH_2	-	1.9 ± 0.6	26 ± 12	29 ± 10
3d[40]	$CH_2C_6H_{11}$	4-Ph-Ph-CH_2		3.5 ± 0.5	73 ± 45	34 ± 8.0
14a	$CH_2C_6H_{11}$	Bn	0	4.8 ± 0.7	36 ± 9.0	3.2 ± 0.4
15a	$CH_2C_6H_{11}$	Bn	0	6.9 ± 1.6	60 ± 26[e]	2.4 ± 0.2
ent-**14a**	$CH_2C_6H_{11}$	Bn	0	23 ± 13	197 ± 18	2.8 ± 1.0
ent-**15a**	$CH_2C_6H_{11}$	Bn	0	5.7 ± 2.6	501 ± 21	1.6 ± 0.4
14b	Me	Bn	0	13%[d]	4%[d]	23%[d]
15b	Me	Bn	0	0%[d]	7%[d]	n.d.
14c	$CH_2C_6H_{11}$	1-Naph-CH_2	0	8.0 ± 2.0	51 ± 16	13 ± 5.0
15c	$CH_2C_6H_{11}$	1-Naph-CH_2	0	7.1 ± 1.8	157 ± 21	7.2 ± 3.9
ent-**14c**	$CH_2C_6H_{11}$	1-Naph-CH_2	0	14 ± 4.0	40 ±15	38 ± 3.0
ent-**15c**	$CH_2C_6H_{11}$	1-Naph-CH_2	0	0.50 ± 0.1[e]	116 ± 33	6.0 ± 2.0
14d	$CH_2C_6H_{11}$	4-Ph-Ph-CH_2	0	8.7 ± 1.2	20 ± 7.0	27 ± 9.0
15d	$CH_2C_6H_{11}$	4-Ph-Ph-CH_2	0	23 ± 6.0	334 ± 18	73 ±6.0
ent-**14d**	$CH_2C_6H_{11}$	4-Ph-Ph-CH_2	0	11 ± 2.0	202 ± 52	27 ± 5.0
ent-**15d**	$CH_2C_6H_{11}$	4-Ph-Ph-CH_2	0	11 ± 2.0	593 ± 53	24 ± 6.0
22a	$CH_2C_6H_{11}$	Bn	1	6.0 ± 0.2	65 ± 7.0	6.4 ± 0.9
23a	$CH_2C_6H_{11}$	Bn	1	1.6 ± 0.1	284 ± 72	2.2 ± 1.1
(+)-pentazocine				5.4 ± 0.5	-	36 ± 5.0
Haloperidol				6.6 ± 0.9	78 ± 2.0	40 ± 5.0
di-*o*-tolylguanidine				71 ± 8.0	58 ± 18	208 ± 26

[a] gp: guinea pig brain; [b] rat liver; [c] RPMI 8226 cell line; [d] Inhibition of radioligand binding at 1 µM concentration of test compound; [e] n = 4; n.d.: not determined. K_i values represent mean values of three independent experiments (n = 3).

The similar σ_1 receptor affinities of the four stereoisomeric benzyl substituted derivatives **14a**, *ent*-**14a**, **15a** and *ent*-**15a** indicate that the configuration has a negligible effect on the interaction with σ_1 receptors. Replacement of the benzyl residue (**a**-series) by the voluminous biphenylylmethyl moiety (**d**-series) results in a slight reduction of σ_1 affinity as shown for the stereoisomers **14d**, *ent*-**14d**, **15d** and *ent*-**15d**. As observed for the benzyl derivatives (**a**-series) the stereochemistry of the biphenylylmethyl derivatives (**d**-series) does not influence the σ_1 affinity, considerably.

Expansion of the ethano bridge by a methylene moiety does not reflect into a considerable change in the σ_1 affinity of the corresponding derivatives. Indeed, the propano bridged homologs **22a** and **23a** show almost the same σ_1 affinity as the ethano bridged ligands **14a** and **15a** with the same stereochemistry and the same substitution pattern.

The σ_2 receptor affinity of all bicyclic compounds is lower than their σ_1 affinity (gp assay, RPMI 8226 assay) varying from slight preference up to a high selectivity for the σ_1 receptor. The range of the σ_1:σ_2 selectivity is demonstrated by the naphthylmethyl derivatives (**c**-series), which show σ_1:σ_2 selectivity of 6, 3, 22, and 230-fold for **14c**, *ent*-**14c**, **15c** and *ent*-**15c**, respectively. The particular high σ_1:σ_2 selectivity of the (1*S*,4*R*,7*S*)-configured ligands *ent*-**15a** (90-fold), *ent*-**15c** (230-fold), and *ent*-**15d** (55-fold) should be emphasized.

The affinity of the bicyclic compounds towards human σ_1 receptors (RPMI 8226 cell line) shows a good correlation to the affinity recorded in the guinea pig brain assay. In general the K_i-values for the naphthylmethyl (**c**-series), biphenylylmethyl

derivatives (**d-**series) and propano bridged homologs **22a** and **23a** are slightly higher in the RPMI 8226 assay than in the guinea pig brain assay. In contrast, the benzyl derivatives (**a**-series) show slightly stronger interactions with the human σ_1 receptor in the RPMI 8226 assay than with the guinea pig σ_1 receptors. However, most of the measured differences are due to the variability of the assays, thus lacking significance. Interestingly, the most potent ligand in the guinea pig assay (*ent*-**15c**, K_i = 0.50 nM) shows also very high affinity in the RPMI 8226 assay (K_i = 6.0 nM) rendering it to one of the most affine ligands in this assay as well.

In conclusion, reduction of the conformational flexibility of (hydroxyethyl)piperazines **3** by incorporation of the pharmacophoric elements in a diazabicyclo[2.2.2]octane framework led to the same or slightly reduced σ_1 affinity. K_i values recorded in the guinea pig assay are in good accordance with K_i values recorded in the RPMI 8226 assay. (1*S*,4*R*,7*S*)-Configured bicyclic ligands display high σ_1:σ_2 selectivity. The ligand *ent*-**15c** represents the most promising σ_1 ligand of this series of bicyclic compounds with K_i values of 0.50 nM (guinea pig assay), 6.0 nM (RPMI 8226 assay) and 230-fold respective 20-fold selectivity over the σ_2 subtype.

Cytotoxicity

The ability of the new σ_1 ligands to inhibit the growth of seven human tumor cell lines was investigated *in vitro* by using two microtiter plate-based assays: the growth of the adherent cell lines A427 (small cell lung cancer), LCLC-103H (large cell lung cancer), 5637 and RT-4 (bladder cancer), DAN-G (pancreatic cancer) and MCF-7 (breast cancer) was determined by a crystal violet staining assay described previously,[52] whilst for the cell line HL60 (leukemia) growing in suspension the MTT assay was

used.[52] The known σ_1 ligands (+)-pentazocine and haloperidol were included in these investigations and served as reference compounds.

Table 2 displays the 50% growth inhibition concentrations (IC_{50}) of the synthesized bicyclic σ ligands **14**, **15**, **22a**, and **23a** together with the effects of the reference compounds (+)-pentazocine and haloperidol. As expected, **15b** bearing a small methyl moiety at N-2 did not inhibit the growth of any of the tumor cell lines up to a concentration of 20 μM. This effect correlates well with its negligible affinity towards both σ receptor subtypes.

The naphthylmethyl substituted derivatives **14c** and **15c** reveal rather unselective inhibition of tumor cell growth based on very similar IC_{50} values over all cell lines, thus indicating unspecific cytotoxicity rather than a precise mechanism of action. Compounds **15a**, *ent*-**14a**, *ent*-**15c**, and **14d** slightly reduced the growth of the bladder cancer cell line 5637. However, the most striking result is the selective growth inhibition of the small cell lung cancer cell line A427 by the cyclohexylmethyl substituted bicyclic compounds (exception made for **14c** and **15c**, which are not selective). The growth of the other five cell lines was not influenced up to a test compound concentration of 10 μM or 20 μM. Therefore, the following discussion will focus on the growth inhibition of tumor cell line A427, which expresses high levels of σ_1 receptors[37] and is the most sensitive cell line towards these bicyclic ligands.

Table 2: Growth inhibition of human tumor cell lines, average IC_{50} ± SD [µM] of three independent determinations (except where noted)

compd.	human tumor cell line						
	A427[a]	LCLC-103H[a]	5637[a]	RT-4[a]	DAN-G[a]	MCF-7[a]	HL60[b]
14a	16.5 ± 6.2	> 20	> 20	> 20	> 20	> 20	> 20
15a	9.8 ± 4.3	> 20	9.2 ± 6.3	> 20	> 20	> 20	> 20
ent-**14a**	2.8 ± 1.7	> 20	4.8 ± 3.1	> 20	> 20	> 20	> 20
ent-**15a**	11.2 ± 4.8	> 20	> 20	> 20	> 20	> 20	> 20
14b	n.d.	n.d.	n.d.	n.d.	n.d.	n.d.	n.d.
15b	> 20	> 20	> 20	> 20	> 20	> 20	n.d.[c]
14c	2.3 ± 0.9	10.4 ± 0.9	4.3 ± 1.8	12.9 ± 7.3	10.2 ± 3.1	7.0 ± 4.1	11.2 ± 1.6
15c	6.0 ± 3.8	8.8 ± 2.0	4.9 ± 1.2	11.3 ± 5.9	16.1 ± 2.1	6.8 ± 1.5	14.7 ± 1.4
ent-**14c**	1.8[e)]	> 10	> 10	n.d.	9.3[e)]	n.d.	n.d.
ent-**15c**	4.3 ± 2.3	> 10	2.3 ± 0.9	n.d.	> 10	n.d.	n.d.
14d	1.6 ± 1.2	3.2[e)]	4.9 ± 4.1	n.d.	4.9 ± 2.0	n.d.	n.d.
15d	4.5 ± 5.7	> 10	> 10	n.d.	> 10	n.d.	n.d.
ent-**14d**	3.7 ± 3.6	> 10	> 10	n.d.	9.1 ± 1.0	n.d.	n.d.
ent-**15d**	1.9 ± 1.5	> 10	> 10	n.d.	> 10	n.d.	n.d.
22a	7.6 ± 4.7	> 20	> 20	> 20	> 20	14 ± 2.8	> 20
23a	10.3 ± 2.9	> 20	> 20	> 20	> 20	16 ± 2.8	> 20
+)-pentazocine	> 20	> 20	3.5 ± 0.9	> 20[d]	> 20	> 20[d]	> 20
Haloperidol	9.6 ± 3.7	10.9 ± 1.9	2.3 ± 1.4	16 ± 5[d]	> 20	> 20[d]	> 20

[a)]determined with the crystal violet assay after a 96 h exposure to test compounds; [b)]determined with the MTT assay after a 48 h exposure of the HL60 cell line to test compounds; [c)]n.d.: not determined, [d)]values from ref.[37], [e)]n = 2

As discussed for the σ_1 receptor affinity, the four stereoisomeric cyclohexylmethyl derivatives **14a**, *ent*-**14a**, **15a** and *ent*-**15a** display very similar antiproliferative activity against A427 cell line, indicating a low influence of the stereochemistry on cell growth inhibition. Similar observations were made for the growth inhibition of the

stereoisomeric naphthylmethyl (**c**-series) and biphenylylmethyl (**d**-series) substituted derivatives as well as for enantiomeric monocyclic piperazine derivatives.[54] The most potent compounds are the naphthylmethyl substituted compounds **14c** (IC_{50} = 2.3 µM) and *ent*-**14c** (IC_{50} = 1.8 µM) as well as the biphenylylmethyl substituted derivatives **14d** (IC_{50} = 2.3 µM) and *ent*-**15d** (IC_{50} = 1.9 µM). With K_i values of 13 nM (**14c**) and 27 nM (**14d**) in the human RPMI8226 assay, the (1*R*,4*S*,7*S*)-configured compounds belong to the group of very high affinity σ_1 ligands. Although a precise correlation between the antiproliferative activity against the A427 cell line and the σ_1 affinity is not given, the high affinity σ_1 ligands *ent*-**14a** (K_i(human) = 2.8 nM) and *ent*-**15c** (K_i(human) = 6.0 nM) inhibit the growth of the A427 tumor cell line also with high activity (IC_{50} = 2.8 µM (*ent*-**14a**), IC_{50} = 4.3 µM (*ent*-**15c**)).

The size of the bridge does not influence considerably the growth inhibition of the A427 cell line, since the homologs **22a** and **23a** with an additional CH_2 moiety in the bridge show similar antiproliferative activity as their smaller homologs **14a** and **15a**.

It can be concluded that a clear correlation between the σ_1 affinity of the test compounds and their antiproliferative activities in the A427 cell line could not be detected, but some trends were observed. For the interpretation of these results it has to be considered that some physico-chemical properties of the test compounds, such as lipophilicity, which determine penetration of drugs through the cytoplasmic membrane to enter the cells and interact with σ_1 receptors located in the membrane of the endoplasmic reticulum, influence the overall effect on tumor cell growth. These aspects are not relevant in receptor binding studies with membrane preparations. However, all bicyclic compounds bearing a cyclohexylmethyl moiety behave like the σ_1 receptor antagonist haloperidol in the inhibition of the growth of the A427 cell line.

Therefore, the bicyclic compounds are likely to also be acting as σ_1 receptor antagonists.

Induction of apoptosis

Based on their σ_1 affinity and tumor cell growth inhibition, the bicyclic 5-benzyl derivative *ent*-**14a** (**a**-series), the naphthylmethyl derivatives *ent*-**14c** and *ent*-**15c** (**c**-series), and the biphenylylmethyl derivative *ent*-**14d** (**d**-series) were selected for further investigation of apoptosis induction in A427 cells (small cell lung cancer). This human tumor cell line displays a high expression of σ_1 receptors[37] and a high sensitivity towards cytotoxic effects of the compounds (Table 2). Cells were treated for 24 h and 48 h with a 2-fold higher concentration of the compounds than the corresponding IC_{50} value, established by the crystal violet proliferation assay (96 h). Subsequently the cells were double-stained with annexin V-FITC and propidium iodide (PI) to distinguish between early apoptotic and late apoptotic/necrotic cells. The stained cells were analyzed by flow cytometry. The anticancer agent doxorubicin (0.5 µM for 24 h, 0.1 µM for 48 h), a well-known inducer of apoptosis[55,56], was included as a positive control.

The results of the annexin V / PI double staining experiments are shown in Figure 2. Whilst after 24,h significant increases in the population of early apoptotic cells (annexin V-positive, PI-negative) could only be observed for the biphenylylmethyl derivative *ent*-**14d** (39.7 ± 1.3 %), after 48 h the fraction of early apoptotic cells significantly increased for all four of the tested compounds (*ent*-**14a**: 32.6 ± 1.5 % , *ent*-**14c**: 33.3 ± 5.4 %, *ent*-**15c**: 48.9 ± 3.8 %, *ent*-**14d**: 56.4 ± 4.3 %) compared to a 0.1 % (v/v) DMSO-containing solvent control (19.0 ± 2.5 % after 24 h, 17.3 ± 1.8 % after 48 h). Untreated cells (medium only) displayed similar fractions of early

apoptotic cells (18.9 ± 2.8 % after 24 h, 16.6 ± 1.1 % after 48 h). Thus, for these four compounds, the biphenylylmethyl derivative *ent*-**14d** with high σ_1 affinity (K_i = 11 nM) and growth inhibition (IC_{50} (A427) = 3.7 µM) is the most effective and fastest inducer of apoptosis in A427 cells. Comparable time-dependent induction of apoptosis by σ_1 ligands with hydroxyethyl framework (see **3** in Figure 1) has been observed before.[40,54]

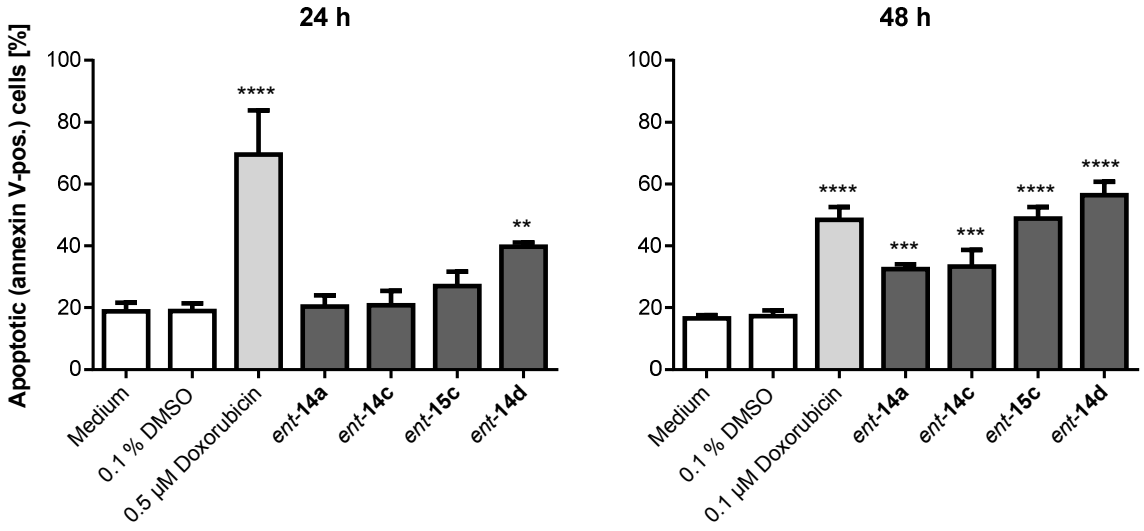

Figure 2: Analysis of apoptotic effects of *ent*-**14a**, *ent*-**14c**, *ent*-**15c** and *ent*-**14d** by annexin V / PI double staining. Annexin V-positive and PI-negative A427 cells after treatment with *ent*-**14a** (5.6 µM), *ent*-**14c** (3.4 µM), *ent*-**15c** (8.7 µM), and *ent*-**14d** (7.4 µM) for 24 h and 48 h, respectively. Apoptosis was evaluated by flow cytometry by determining the percentage of annexin V-positive, PI-negative cells. Results expressed as mean ± SD [µM] of at least three independent experiments. Doxorubicin (0.5 µM for 24 h, 0.1 µM for 48 h) as positive control, 0.1 % (v/v) DMSO as solvent negative control. * $p \leq 0.05$, ** $p \leq 0.01$, *** $p \leq 0.001$, **** $p < 0.0001$ (two-way ANOVA followed by Dunnett's multiple comparisons test by using GraphPad Prism, GraphPad Software)

Molecular simulations

With the purpose of explaining the interactions between this new series of bridged piperazines and the σ_1 receptor at the molecular level, all derivatives were docked in the binding site of our 3D homology model[38,40,57] and the corresponding

ligand/protein free energies of binding (ΔG_{bind})[58-61] were evaluated by applying a molecular dynamics (MD)-based scoring procedure in the framework of the so-called Molecular Mechanics/Poisson-Boltzannn Surface Area (MM/PBSA) approach.[62] Further, we performed a per-residue decomposition of the enthalpic component of ΔG_{bind}[58-61] in order to quantitatively identify contribution afforded by the σ_1 amino acids mainly involved in binding these bicyclic compounds.

The analysis of the MD trajectories reveals that the new derivatives can establish a series of intermolecular interactions quite similar to those previously detected for the more flexible (ω-hydroxyalkyl)piperazines **1** and **3**.[40] Actually, all new synthesized σ_1 ligands can bind their target receptor by exploiting four highly specific molecular determinants, schematically represented in Figure 3A. In details, the cyclohexylmethyl substituent at N-2 of the diazabicyclic system is encased in the hydrophobic pocket generated by the σ_1 residues Ile128, Phe133, Tyr173, and Leu186, thereby establishing favorable, hydrophobic interactions with their side chains. The basic N-arylmethyl nitrogen atom (N-5) is engaged in a permanent salt bridge with the carboxylic group of Asp126 whilst the different arylmethyl moieties, common to all these new derivatives, are anchored in place by stabilizing π-type interactions. Specifically, residues Arg119 and Tyr120 are involved in receptor/ligand π-cation and π-π interactions, respectively (see Figure 3A). Finally, the hydroxy substituent present on one of the three chiral carbon atoms of the diazabicyclic scaffold plays an important functional group in the structure of these new molecules. Indeed, it serves as a hydrogen bond acceptor, the donor counterpart being the –OH group of the Thr181 side chain. The general binding mode of the new ligands

described above is portrayed in details in Figure 3B, taking compound **14d** as a proof-of-concept.

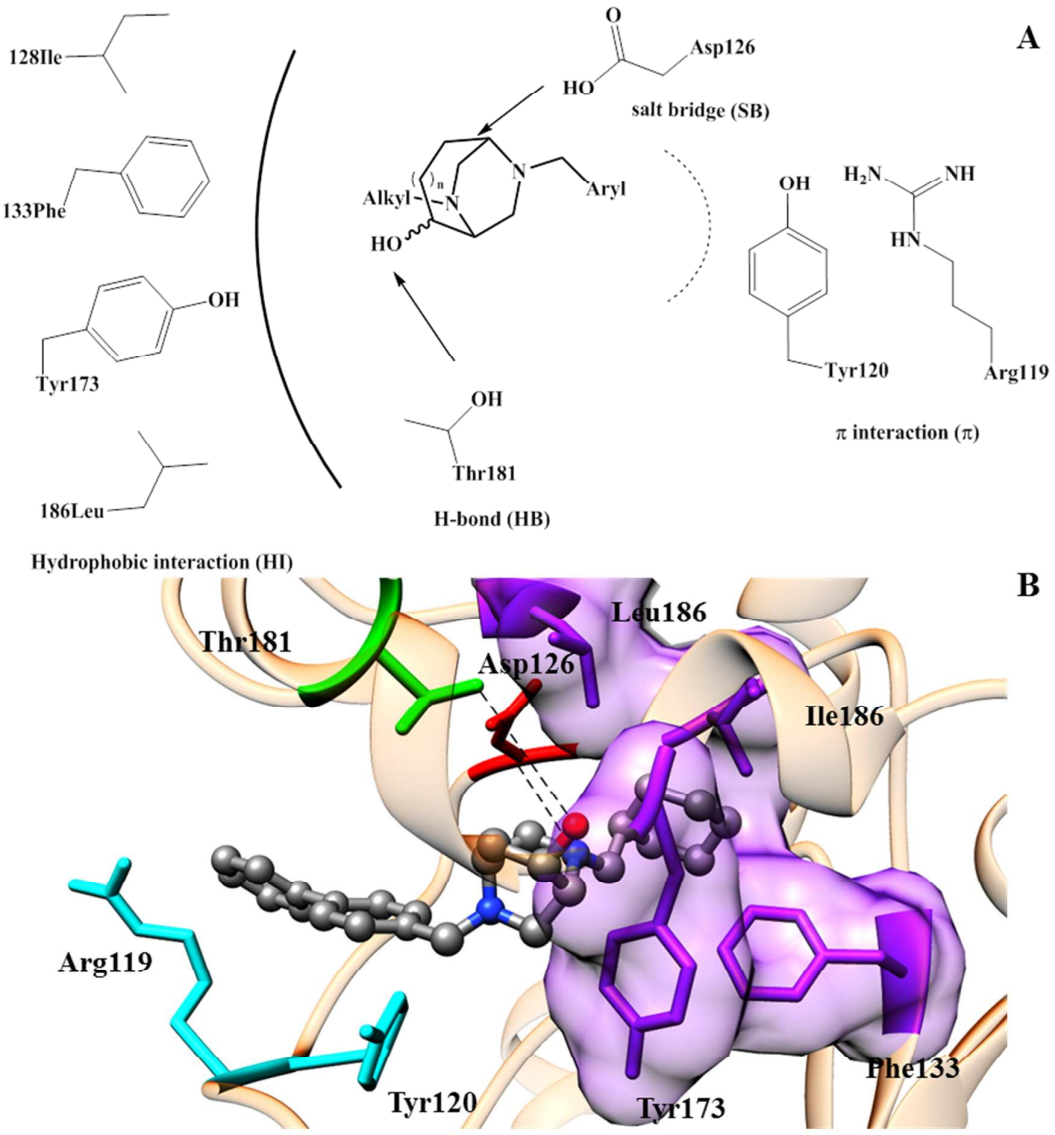

Figure 3. (A) 2D schematic representation of the identified interactions between the 3D homology model of the σ_1 receptor and the bicyclooctane(-nonane) compounds synthesized in this work. The lines/arrows indicate key interactions between the receptor and its ligand. (B) Equilibrated MD snapshot of the complex of the σ_1 receptor with compound **14d**. The main protein residues involved in these interactions are Arg119 and Tyr120 (π-interactions, cyan), Asp126 (salt bridge, red), Ile128, Phe133, Tyr173, and Leu186 (hydrophobic interactions, purple), and Thr181 (hydrogen bond, green). Compound **14d** is shown in atom-colored sticks-and-balls (C, gray; N, blue; and O, red). H atoms are omitted, but the salt bridge and the H-bond are indicated as black dotted lines. Water molecules, ions, and counterions are not shown for clarity.

Table 3. MM/PBSA calculated binding enthalpy (ΔH_{bind}), binding entropy ($-T\Delta S_{bind}$), binding free energy (ΔG_{bind}), and the calculated K_i values for all compounds considered in this work. The corresponding experimental values (Table 1) are also shown in the last column for comparison.

	ΔH_{bind} [kcal/mol]	$-T\Delta S_{bind}$ [kcal/mol]	ΔG_{bind} [kcal/mol]	σ_1 (calcd) K_i [nM][a)]	σ_1 (hum) K_i ± SEM [nM]
3a	-22.19 (0.16)	-12.01 (0.28)	-10.18 (0.32)	21	21 ± 4.0
3b	-17.44 (0.15)	-10.40 (0.31)	-7.04 (0.34)	6900	n.d.
3c	-23.34 (0.17)	-12.62 (0.27)	-10.72 (0.43)	14	29 ± 10
3d	-23.31 (0.18)	-13.02 (0.29)	-10.29 (0.34)	29	34 ± 8.0
14a	-20.68 (0.21)	-10.15 (0.28)	-10.53 (0.35)	19	3.2 ± 0.4
15a	-20.63 (0.16)	-10.18 (0.29)	-10.45 (0.33)	22	2.4 ± 0.2
ent-**14a**	-20.90 (0.17)	-10.09 (0.31)	-10.81 (0.35)	12	2.8 ± 1.0
ent-**15a**	-21.14 (0.21)	-10.21 (0.27)	-10.93 (0.34)	9.7	1.6 ± 0.4
14b	-17.45 (0.20)	-9.99 (0.30)	-7.46 (0.38)	3400	23%[d)]
15b	-17.27 (0.19)	-9.86 (0.34)	-7.41 (0.39)	3700	n.d.
14c	-21.52 (0.16)	-10.33 (0.28)	-11.19 (0.32)	6.3	13 ± 5.0
15c	-21.25 (0.18)	-10.24 (0.29)	-11.01 (0.34)	8.5	7.2 ± 3.9
ent-**14c**	-21.80 (0.22)	-10.42 (0.26)	-11.38 (0.34)	4.6	38 ± 3.0
ent-**15c**	-21.85 (0.21)	-10.39 (0.29)	-11.46 (0.36)	4.0	6.0 ± 2.0
14d	-21. 21 (0.18)	-10.53 (0.30)	-10.68 (0.35)	15	27 ± 9.0
15d	-21.02 (0.21)	-10.46 (0.28)	-10.56 (0.35)	18	73 ± 6.0
ent-**14d**	-20.54 (0.15)	-10.21 (0.28)	-10.33 (0.31)	27	27 ± 5.0
ent-**15d**	-21.02 (0.17)	-10.78 (0.31)	-10.24 (0.35)	31	24 ± 6.0
22a	-20.51 (0.23)	-10.01 (0.29)	-10.50 (0.37)	20	6.4 ± 0.9
23a	-20.58 (0.19)	-9.98 (0.27)	-10.60 (0.33)	17	2.2 ± 1.1

[a)]The σ_1 K_i values were obtained from the corresponding ΔG_{bind} values using the relationship: $\Delta G_{bind} = -RT \ln K_i$.

The MM/PBSA estimated values of the free energy of binding ΔG_{bind} shown in Table 3 confirm that all bicyclic derivatives – with the notable exception of the N-methyl substituted molecules **3b**, **14b** and **15b** (*vide infra*) - are endowed with high affinity toward the σ_1 receptor, since the extrapolated σ_1 K_i values are in nanomolar range.

The per residue deconvolution of the enthalpic contribution to ligand binding, ΔH_{bind}, allows to derive two further, important structural considerations about this new series of compounds within the receptor binding site: the role of a bulky cycloalkyl substituent and the absolute configuration related to the specific stereochemistry of these molecules.

Concerning the first point, the replacement of the cyclohexylmethyl moiety with the considerably smaller methyl group in compounds **14b** and **15b** leads to a dramatic decrease in the relevant σ_1 affinity, quantified by a three orders of magnitude plummet in the corresponding σ_1 K_i values (Tables 1 and 3). The reasons for this behavior can be directly attributed to the reduced efficiency of the methyl substituent, with respect to the bulkier cyclohexyl moiety, in generating substantial hydrophobic connection with the residues lining the receptor binding pocket. This is clearly supported by the relevant interaction spectra shown in Figure 4. *De facto*, the favorable interactions between the cyclohexyl group and the side chains of Ile128, Phe133, Tyr173, and Leu186 amount to ~ 3.5 kcal/mol for the corresponding derivatives while, in the presence of the methyl group, the same interactions barely afford an energetic stabilization to the receptor/ligand complex of 0.75 kcal/mol. This, in turn, exerts a negative effect on global binding conformation of derivatives **14b** and **15b,** ultimately resulting in a general decrement of all enthalpic contributions to ligand binding (Figure 4). In addition, the same analysis confirms that the addition of one

methylene moiety in the cyclic structure (i.e., the diazabicyclononane derivatives **22a** and **23a**) does not result in any significant advantage in the binding of these compounds with the σ_1 receptor, as they exhibit an interaction profile utterly similar to those characterizing the diazabicyclooctane counterparts.

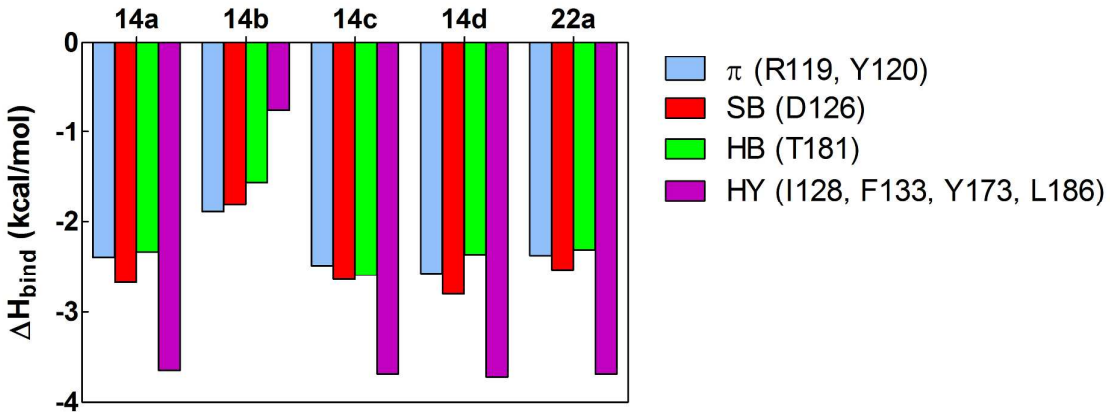

Figure 4. Per residue binding enthalpy decomposition (interaction spectra) for compounds **14a-d** and **22a** in complex with the σ_1 receptor. Only those σ_1 amino acids involved in major intermolecular interactions (see Figure 3) are displayed for simplicity. Legend abbreviations: π = π-type interactions; SB = salt bridge; HB = hydrogen bond; HI = hydrophobic interactions.

Our MD simulation results confirm all present and previous experimental observations regarding the stereochemistry issue: indeed, the flexible nature of the σ_1 binding site enables the receptor to easily and efficiently accommodate each configuration of enantiomeric ligands when these result in small modifications in the orientation of the molecular pharmacophore requirements. Figure 5A clearly shows the obvious similarity in the equilibrated binding poses of the diastereomeric compounds **14d** and **15d,** according to which the relative position of the hydroxy group is practically irrelevant.

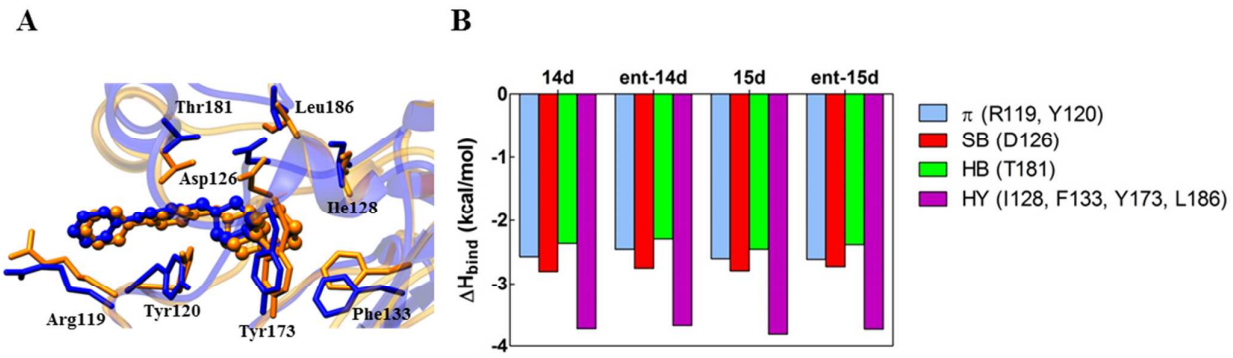

Figure 5. (A) Overlay of binding modes of diastereomers **14d** (orange) and **15d** (blue) in the binding pocket of the σ_1 receptor (colored transparent ribbons). The two ligands are shown as colored sticks-and-balls, whereas the main interacting residues are shown as colored sticks and labelled. Hydrogen atoms, ions, counterions and water molecules are omitted for clarity. (B) Per residue binding enthalpy decomposition (interaction spectra) for compounds **14d**, *ent*-**14d**, **15d**, and *ent*-**15d** in complex with the σ_1 receptor. Only those σ_1 amino acids involved in major intermolecular interactions (see Figures 3 and 4) are shown for simplicity. Legend abbreviations: π = π-type interactions; SB = salt bridge; HB = hydrogen bond; HI = hydrophobic interactions.

Quantitatively speaking, also the corresponding enantiomers *ent*-**14d** and *ent*-**15d** do not display significant differences upon binding to the receptor. In fact, according to the corresponding interaction spectra shown in Figure 5B, all four specific molecular determinants required for stabilizing the relevant σ_1 receptor/ligand complexes are practically not affected as concerns their enthalpic contribution to binding.

Notably, however, even if the new, conformationally more constrained piperazine compounds overall seem to be as potent as the more flexible, monocyclic compounds with respect to σ_1 receptor affinity, this similar behavior is the result of an underlying enthalpy-entropy compensation effect. In fact, as shown in Figure 6, the presence of a substantially more rigid scaffold in the bicyclic derivatives reflects in a less negative (i.e., more favorable) entropic binding component ($-T\Delta S_{bind}$), of ~ 2 kcal/mol compared to the monocyclic compounds **3a**, **3c** and **3d**. On the other hand,

this entropic gain is compensated by a loss of the corresponding enthalpic contribution (ΔH_{bind}). As a net result, the overall ΔG_{bind} values for both molecular series are practically comparable, in harmony with the corresponding, experimental evidences.

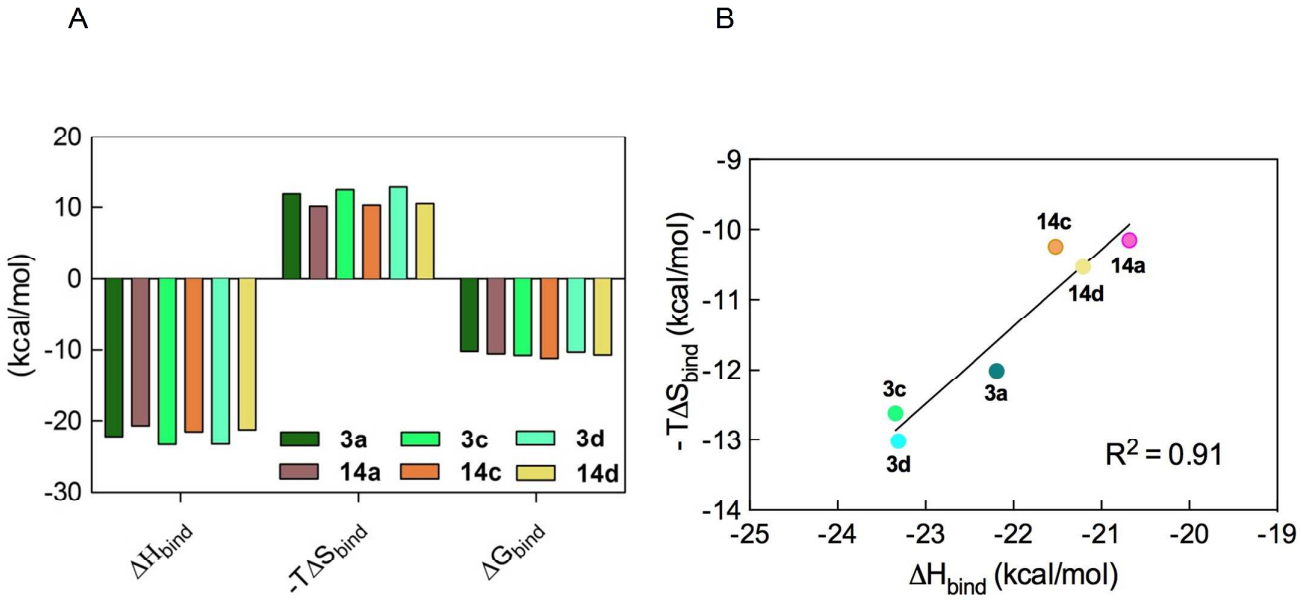

Figure 6. (A): Enthalpy, entropy and free energy of binding for compounds **3a**, **3c** and **3d** and **14a**, **14c**, and **14d**. (B): Enthalpy-entropy compensation graph displaying the enthalpy term (ΔH_{bind}) vs. the entropy term ($-T\Delta S_{bind}$) for the three couples of constrained/uncontrained compounds **3a**/**14a**, **3c**/**14c**, and **3d**/**14d**. The solid line represents the best fit of the data, with $R^2 = 0.91$. Colours are the same as in panel A of Figure 6.

Conclusions

An improved Dieckmann-type cyclization protocol allowed the synthesis of four sets of stereoisomeric 2,5-diazabicyclo[2.2.2]octanes **14a-d** and **15a-d** with different substituents at the N-atoms. Bicyclic compounds **14b** and **15b** with a small methyl substituent at N-2 did not reveal any relevant σ_1 receptor affinity. However, introduction of the large lipophilic cyclohexylmethyl residue at N-2 led to

diazabicyclooctanes **14a**,**c,d** and **15a**,**c,d** binding in the low nanomolar range ($K_i \leq 23$ nM) at σ_1 receptors. The high σ_1 affinity of the cyclohexylmethyl derivatives is explained by favorable interactions of the cyclohexyl group with the side chains of Ile128, Phe133, Tyr173, and Leu186, which amount to ~ 3.5 kcal/mol of binding enthalpy. Interaction of these residues with the small methyl moiety affords only a binding enthalpy of 0.75 kcal/mol, reflecting the reduced affinity. The stereochemistry of the bicyclic compounds has only limited influence on σ_1 receptor binding. Molecular dynamics calculations confirm the adaptation of the flexible σ_1 receptor binding site to stereoisomeric bicyclic ligands resulting in similar binding poses. In particular the orientation of the -OH moiety in the stereoisomers is practically irrelevant. The conformationally restricted derivatives **14a**,**c,d** and **15a**,**c,d** reveal the same or slightly reduced σ_1 affinity as their flexible monocyclic counterparts **3a**,**c,d**. The similar σ_1 affinities are the result of an enthalpy-entropy compensation effect. Whereas the entropic binding component of the bicyclic compounds is increased (~ 2 kcal/mol) the enthalpic component is reduced by approx. the same amount, resulting in comparable binding free enthalpies for both series of ligands.

In order to analyze species differences of σ_1 receptors, membrane preparations obtained from peripheral blood human myeloma cell line RPMI 8226 were used as receptor material in an additional assay and the data were compared with data recorded in the standard guinea pig brain σ_1 assay. In general the affinity data recorded in both assays are well comparable, which reflects the 93% sequence identity of human and guinea pig σ_1 receptors (see Figure S2). The small differences between the values recorded in the assays could be due to the assay conditions. The data recorded in the RPMI 8226 assay are of particular impact since all the molecular

dynamics simulations described herein were performed with the human σ_1 receptor protein.

The growth inhibition of the bicyclic ligands **14**, **15**, **22a** and **23a** against seven human tumor cell lines was investigated. A selective inhibition of the growth of the human small cell lung cancer line A427 was observed, indicating a common mechanism of action. As shown for hydroxyethylpiperazines of type **3** (see Figure 1), the bicyclic ligands induce apoptosis. The biphenylylmethyl derivative *ent*-**14d** was the most effective and fastest inducer of apoptosis in A427 cell lines. Although a clear correlation between the growth inhibition and the σ_1 affinity could not be detected, some common tendencies were found. The most affine σ_1 ligand *ent*-**15c** (K_i(gp) = 0.5 nM; K_i(human) = 6.0 nM) shows high inhibition of the A427 cell growth as well (IC_{50} = 4.3 μM). On the other hand, the very potent antiproliferative compounds **14c** and **14d** display high σ_1 affinity with K_i values of 13 nM and 27 nM, respectively, in the human RPMI8226 σ_1 assay. The antiproliferative effect of the bicyclic compounds supports the σ_1 antagonistic activity of this compound class.

Experimental Part

Chemistry, general

Thin layer chromatography: Silica gel 60 F254 plates (Merck). Flash chromatography (fc): Silica gel 60, 40–43 μm (Merck); parentheses include: diameter of the column, eluent, R_f value. In order to obtain high yields some compounds were adsorbed on silica gel by addition of silica gel to a solution of the compound in an appropriate solvent, removal of the solvent in vacuo and giving the mixture on top of the column. Melting point: Melting point apparatus SMP 3 (Stuart Scientific), uncorrected. ^{1}H NMR (600 MHz, 400 MHz), ^{13}C NMR (151 MHz, 100 MHz): Agilent 600-MR, Agilent

400-MR and Mercury Plus AS 400 NMR spectrometer (Varian); δ in ppm related to tetramethylsilane; coupling constants are given with 0.5 Hz resolution; the assignments of ^{13}C and ^{1}H NMR signals were supported by 2D NMR techniques. The purity of all compounds was determined by HPLC analysis. HPLC (method ACN): Merck Hitachi Equipment; UV detector: L-7400; autosampler:L-7200; pump: L-7100; degasser: L-7614; column: LiChrospher® 60 RP-select B (5 µm); LiCroCART® 250-4 mm cartridge; flow rate: 1.0 mL/min; injection volume: 5.0 µL; detection at λ = 210 nm; solvent A: demineralized H_2O with 0.05% (v/v) trifluoroacetic acid; solvent B: acetonitrile with 0.05% (v/v) trifluoroacetic acid: gradient elution (% A): 0-4 min: 90.0%; 4-29 min: gradient from 90% to 0%; 29-31 min: 0%; 31-31.5 min: gradient from 0% to 90.0%; 31.5-40 min: 90%. According to HPLC analysis the purity of all test compounds is >95%.

(*S*)-2-[1-Benzyl-4-(cyclohexylmethyl)-3,6-dioxopiperazin-2-yl]-*N*-methoxy-*N*-methylacetamide (9a)

N,*O*-Dimethylhydroxylamine hydrochloride (393 mg, 4.0 mmol) was dissolved in CH_2Cl_2 abs (12 mL) and cooled to 0 °C. Trimethylaluminium solution (2 M in toluene, 2 mL, 4.0 mmol) was added and the mixture was stirred at room temperature for 30 min. Then a solution of **8a** (500 mg, 1.3 mmol) in CH_2Cl_2 abs (5 mL) was added and the reaction mixture was stirred for 5 h at room temperature. For work-up, the mixture was filled up with aqueous sodium potassium tartrate solution (10%, 7 mL) and stirred for additional 1 h. The resulting suspension was filtered through Celite and washed with CH_2Cl_2 for several times. The filtrate was concentrated under reduced pressure and the residue was purified by fc (∅ 3 cm, h = 18 cm, v = 20 mL, C_6H_{12}/EtOAc = 1/1, R_f = 0.12). Colorless solid, mp 92 – 95 °C, yield 340 mg (63%). $C_{22}H_{31}N_3O_4$, M_r = 401.4. ^{1}H NMR ($CDCl_3$): δ = 0.89-1.00 (m, 2H, $NCH_2C_6H_{11}$), 1.12-

1.29 (m, 3H, $NCH_2C_6H_{11}$), 1.61-1.71 (m, 6H, $NCH_2C_6H_{11}$), 2.95 (dd, J = 17.7, 3.8 Hz, 1H, $CHCH_2CON(OCH_3)CH_3$), 3.06 (dd, J = 17.7, 3.8 Hz, 1H, $CHCH_2CON(OCH_3)CH_3$), 3.13 (dd, J = 13.5, 7.3 Hz, 1H, $NCH_2C_6H_{11}$), 3.16 (s, 3H, NCH_3), 3.22 (dd, J = 13.5, 6.9 Hz, 1H, $NCH_2C_6H_{11}$), 3.46 (s, 3H, $NOCH_3$), 3.92 (d, J = 17.0 Hz, 1H, $O=CCH_2N$), 4.15 (t, J = 3.9 Hz, 1H, $CHCH_2C$ $ON(OCH_3)CH_3$, 4.40 (d, J = 15.4 Hz, 1H, NCH_2Ar), 4.42 (d, J = 16.9 Hz, 1H, $O=CCH_2N$), 4.91 (d, J = 15.1 Hz, 1H, NCH_2Ar), 7.19-7.36 (m, 5H, Ar-*H*).

(*S*)-2-[1-Benzyl-4-(cyclohexylmethyl)-3,6-dioxopiperazin-2-yl]acetaldehyde (11a)

Under N_2, **9a** (200 mg, 0.50 mmol) was dissolved in THF abs. (10 mL) and cooled down to -78°C. At this temperature, 1.5 equivalents of $LiAlH_4$ solution (1 M in THF, 0.75 ml, 0.75 mmol) were added slowly and the mixture was stirred for 16 h. For work-up, the mixture was treated with HCl (1 M, 6 mL) and warmed to room temperature. The aqueous layer was extracted with Et_2O (5 x 10 mL). The combined organic layers were dried (Na_2SO_4) and the solvent was removed in vacuo (H_2O bath temperature ≤ 30 °C). The crude product was purified by fc (∅ 3 cm, h = 20 cm, v = 20 mL, C_6H_{12}/EtOAc = 1/1, R_f = 0.23). Colorless solid, mp 99 – 102 °C, yield 109 mg (64%). $C_{20}H_{26}N_2O_3$, M_r = 342.4. ^{1}H NMR ($CDCl_3$): δ = 0.90-0.98 (m, 2H, $NCH_2C_6H_{11}$), 1.00 – 1.22 (m, 3H, $NCH_2C_6H_{11}$), 1.64-1.75 (m, 6H, $NCH_2C_6H_{11}$), 2.92 (ddd, J = 18.7, 5.1, 0.9 Hz, 1H, $CHCH_2CHO$), 3.08 (dd, J = 18.6, 4.0 Hz, 1H, $CHCH_2CHO$), 3.16 (dd, J = 13.5, 6.8 Hz, 1H, $NCH_2C_6H_{11}$), 3.30 (dd, J = 13.5, 7.8 Hz, 1H, $NCH_2C_6H_{11}$), 3.96 (d, J = 17.3 Hz, 1H, $O=CCH_2N$), 4.12 (t, J = 4.5 Hz, 1H, $CHCH_2CHO$), 4.35 (d, J = 15.1 Hz, 1H, NCH_2Ar), 4.42 (d, J = 17.2 Hz, 1H $O=CCH_2N$), 4.89 (d, J = 15.2 Hz, 1H, NCH_2Ar), 7.20-7-35 (m, 5H, Ar-*H*), 9.52 (s, 1H, C*H*O).

(1*S*,4*S*,7*R*)-5-Benzyl-2-(cyclohexylmethyl)-7-methoxy-7-(trimethylsilyloxy)-2,5-diazabicyclo[2.2.2]octane-3,6-dione (12a)

Under N_2, **8a** (2.68 g, 7.2 mmol) was dissolved in THF abs (50 mL) and the mixture was cooled down to -78 °C. Then a 1 M solution of sodium hexamethyldisilazane in THF (21.6 mL, 21.6 mmol) was added dropwise. After stirring at -78 °C for 40 min, the mixture was treated with chlorotrimethylsilane (2.27 mL, 18.0 mmol) and stirred for additional 1 h at -78 °C and at room temperature for 2 h. Then, an aqueous solution of $NaHCO_3$ (35 mL) was added and the mixture was extracted with CH_2Cl_2 (3 x 25 mL). The combined organic layers were dried (Na_2SO_4), filtered and concentrated in vacuo. The residue was adsorbed on silica gel and given on a silica column (∅ 5.5 cm, h = 20 cm, v = 65 mL, C_6H_{12}/EtOAc = 4/1, R_f = 0.39). Colorless solid, mp 138 – 141 °C, yield 540 mg (17%). $C_{24}H_{36}N_2O_4Si$, M_r = 444.5. ^{1}H NMR ($CDCl_3$): δ = 0.20 (s, 9H, $OSi(CH_3)_3$), 0.85-0.96 (m, 2H, $NCH_2C_6H_{11}$), 1.08-1.27 (m, 3H, $NCH_2C_6H_{11}$), 1.51-1.72 (m, 6H, $NCH_2C_6H_{11}$), 1.84 (dd, J = 13.6, 3.9 Hz, 1H, 8-*H*), 2.07 (dd, J = 13.6, 2.0 Hz, 1H, 8-*H*), 2.74 (dd, J = 13.8, 6.6 Hz, 1H, $NCH_2C_6H_{11}$), 3.21 (s, 3H, OCH_3), 3.60 (dd, J = 13.8, 7.7 Hz, 1H, $NCH_2C_6H_{11}$), 3.82 (dd, J = 3.9, 2.0 Hz, 1H, 4-*H*), 3.95 (s, 1H, 1-*H*), 4.25 (d, J = 14.8 Hz, 1H, NCH_2Ar), 4.83 (d, J = 14.8 Hz, 1H, NCH_2Ar), 7.24-7.34 (m, 5H, Ar-*H*).

(1*S*,4*S*)-5-Benzyl-2-(cyclohexylmethyl)-2,5-diazabicyclo[2.2.2]octane-3,6,7-trione (13a)

12a (450 mg, 1.0 mmol) was dissolved in a mixture of THF/0.5 M HCl (9/1, 150 mL) and the reaction mixture was stirred for 16 h at room temperature. For work-up, H_2O was added (12 mL) and the mixture was extracted with CH_2Cl_2 (3 x 25 mL). The combined organic layers were dried (Na_2SO_4), filtered and the solvent was removed in vacuo. The residue was adsorbed on silica gel and given on a silica column (∅ 3

cm, h = 18 cm, v = 20 mL, C_6H_{12}/EtOAc = 3/2, R_f = 0.23). Colorless solid, mp 151 – 155 °C, yield 339 mg (99%). $C_{20}H_{24}N_2O_3$, M_r = 340.4. ^{1}H NMR ($CDCl_3$): δ = 0.84-0.95 (m, 2H, $NCH_2C_6H_{11}$), 1.07-1.25 (m, 3H, $NCH_2C_6H_{11}$), 1.51-1.71 (m, 6H, $NCH_2C_6H_{11}$), 2.20 (dd, J = 18.6, 3.3 Hz, 1H, 8-*H*), 2.52 (dd, J = 18.5, 2.1 Hz, 1H, 8-*H*), 3.16 (dd, J = 13.9, 6.9 Hz, 1H, $NCH_2C_6H_{11}$), 3.36 (dd, J = 13.9, 6.8 Hz, 1H, $NCH_2C_6H_{11}$), 4.11 (dd, J = 3.3, 2.1 Hz, 1H, 4-*H*), 4.21 (s, 1H, 1-*H*), 4.37 (d, J = 14.6 Hz, 1H, NCH_2Ar), 4.89 (d, J = 14.6 Hz, 1H, NCH_2Ar), 7.23-7.33 (m, 5H, Ar-*H*).

(1*R*,4*S*,7*S*)-5-Benzyl-2-(cyclohexylmethyl)-2,5-diazabicyclo[2.2.2]octan-7-ol (14a) and (1*R*,4*S*,7*R*)-5-Benzyl-2-(cyclohexylmethyl)-2,5-diazabicyclo[2.2.2]octan-7-ol (15a)

13a (310 mg, 0.91 mmol) was dissolved in THF abs. (30 mL) and the mixture was cooled down to 0 °C. At this temperature, $LiAlH_4$ solution (1M in THF, 5.46 mL, 5.46 mmol) was added. The reaction mixture was stirred at 0 °C for 10 min and then heated to reflux for 16 h. Finally H_2O was added under ice-cooling until H_2-liberation was finished. The mixture was stirred at 0 °C for 10 min and then heated to reflux for 30 min. After cooling to room temperature, the mixture was filtered and the solvent was removed in vacuo. The crude product was purified by fc (∅ 3 cm, h = 20 cm, v = 10 mL, C_6H_{12}/EtOAc = 9.5/0.5 + 0.5% *N*,*N*-dimethylethylamine). $C_{20}H_{30}N_2O$, M_r = 314.5.

14a: (R_f = 0.49). Colorless solid, mp 68 – 72 °C, yield 45.8 mg (16%). ^{1}H NMR ($CDCl_3$): δ = 0.84-0.94 (m, 2H, $NCH_2C_6H_{11}$), 1.14-1.29 (m, 4H, $NCH_2C_6H_{11}$), 1.38-1.43 (m, 2H, $NCH_2C_6H_{11}$, 8-*H*), 1.68-1.74 (m, 4H, $NCH_2C_6H_{11}$), 1.87 (d, J = 13.5 Hz, 1H, O-*H*), 2.29 (dd, J = 11.8, 8.8 Hz, 1H, $NCH_2C_6H_{11}$), 2.37-2.44 (m, 1H, 8-*H*), 2.51-2.55 (m, 2H, $NCH_2C_6H_{11}$, 4-*H*), 2.58-2.62 (m, 2H, NCH_2, 1-*H*), 2.72 (dt, J = 10.2, 2.2 Hz, 1H, NCH_2), 2.98, 3.07 (m, 2H, NCH_2), 3.60 (d, J = 13.4 Hz, 1H, NCH_2Ar), 3.64 (d,

J = 13.1 Hz, 1H, NC*H*$_2$Ar), 3.92 (dt, J = 8.8, 2.8 Hz, 1H, 7-*H*), 7.21-7.36 (m, 5H, Ar-*H*).

15a: (R_f = 0.36). Colorless oil, yield 119.7 mg (42%). ^{1}H NMR ($CDCl_3$): δ = 0.78-0.91 (m, 2H, $NCH_2C_6H_{11}$), 1.13-1.20 (m, 3H, $NCH_2C_6H_{11}$), 1.31-1.42 (m, 1H, $NCH_2C_6H_{11}$), 1.65-1.80 (m, 6H, $NCH_2C_6H_{11}$, 8-*H*), 2.10 (ddd, J = 13.7, 8.8, 1.7 Hz, 1H, 8-*H*), 2.34 (dd, J = 11.8, 6.7 Hz, 1H, NC*H*$_2$C$_6$H$_{11}$), 2.41 (dd, J = 11.8, 6.7 Hz, 1H, NC*H*$_2$C$_6$H$_{11}$), 2.62-2.65 (m, 2H, NC*H*$_2$, 4-*H*), 2.66-2.69 (m, 1H, 1-*H*), 2.74-2.78 (m, 2H, NC*H*$_2$), 3.08 (dd, J = 10.8, 2.9 Hz, 1H, NC*H*$_2$), 3.64 (d, J = 14.0 Hz, 1H, NC*H*$_2$Ar), 3.67 (d, J = 13.7 Hz, 1H, NC*H*$_2$Ar), 4.03-4.07 (m, 1H, 7-*H*), 7.21-7.35 (m, 5H, Ar-*H*). The signal for the proton of the OH group is not seen.

(1*S*,2*R*,5*S*)-6-Benzyl-8-(cyclohexylmethyl)-2-methoxy-2-(trimethylsilyloxy)-6,8-diazabicyclo[3.2.2]nonane-7,9-dione (20)

Under N_2, **19** (980 mg, 2.5 mmol) was dissolved in THF abs (50 mL) and the mixture was cooled down to -78 °C. Then a 1 M solution of sodium hexamethyldisilazane in THF (7.6 mL, 7.6 mmol) was added dropwise. After stirring at -78 °C for 40 min, the mixture was treated with chlorotrimethylsilane (0.8 mL, 6.3 mmol) and stirred for additional 1 h at -78 °C and at room temperature for 2 h. Then an aqueous solution of $NaHCO_3$ (20 mL) was added and the mixture was extracted with CH_2Cl_2 (3 x 15 mL). The combined organic layers were dried (Na_2SO_4), filtered and concentrated in vacuo. The residue was adsorbed on silica gel and given on a silica column (∅ 5 cm, h = 22 cm, v = 65 mL, C_6H_{12}/EtOAc = 8.5/1.5, R_f = 0.22). Colorless solid, mp 112 – 113 °C, yield 698 mg (61%). $C_{25}H_{38}N_2O_4Si$, M_r = 458.7. ^{1}H NMR ($CDCl_3$): δ = 0.21 (s, 9H, $OSi(CH_3)_3$), 0.86-0.99 (m, 2H, $NCH_2C_6H_{11}$, 3-*H*, 4-*H*), 1.13-1.26 (m, 3H, $NCH_2C_6H_{11}$, 3-*H*, 4-*H*), 1.45-1.51 (m, 1H, $NCH_2C_6H_{11}$, 3-*H*, 4-*H*), 1.55-1.75 (m, 6H, $NCH_2C_6H_{11}$, 3-*H*, 4-*H*), 1.80-1.89 (m, 3H, $NCH_2C_6H_{11}$, 3-*H*, 4-*H*), 2.69 (dd, J = 13.6,

6.3 Hz, 1H, NCH_2C$_6$H$_{11}$), 3.24 (s, 3H, OCH_3), 3.77 (dd, J = 13.7, 7.7 Hz, 1H, NCH_2C$_6$H$_{11}$), 3.81-3.83 (m, 1H, 5-*H*), 3.95 (s, 1H, 1-*H*), 4.41 (d, J = 14.6 Hz, 1H, NCH_2Ar), 4.66 (d, J = 14.7 Hz, 1H, NCH_2Ar), 7.23-7.32 (m, 5H, Ar-*H*).

(1*S*,5*S*)-6-Benzyl-8-(cyclohexylmethyl)-6,8-diazabicyclo[3.2.2]nonane-2,7,9-trione (21)

20 (500 mg, 1.1 mmol) was dissolved in a mixture of THF/0.5 M HCl (9/1, 70 mL) and the reaction mixture was stirred for 16 h at room temperature. For work-up, H_2O was added (12 mL) and the mixture was extracted with CH_2Cl_2 (3 x 25 mL). The combined organic layers were dried (Na_2SO_4), filtered and the solvent was removed in vacuo. The residue was adsorbed on silica gel and given on a silica column (∅ 3 cm, h = 16 cm, v = 20 mL, C_6H_{12}/EtOAc = 7/3, R_f = 0.16). Colorless solid, mp 135- -140 °C, yield 354.7 mg (91%). $C_{21}H_{26}N_2O_3$, M_r = 354.4. ^{1}H NMR ($CDCl_3$): δ = 0.87-1.02 (m, 2H, NCH$_2$C$_6$*H*$_{11}$), 1.12-1.26 (m, 3H, NCH$_2$C$_6$*H*$_{11}$), 1.54-1.73 (m, 6H, NCH$_2$C$_6$*H*$_{11}$), 2.82-2.34 (m, 1H, 4-*H*), 2.46-2.51 (m, 1H, 4-*H*), 2.48 (ddd, J = 15.6, 7.2, 4.3 Hz, 1H, 3-*H*), 2.74 (dt, J = 15.6, 8.4 Hz, 1H, 3-*H*), 2.92 (dd, J = 13.8, 6.5 Hz, 1H, NCH_2C$_6$H$_{11}$), 3.61 (dd, J = 13.8, 7.4 Hz, 1H, NCH_2C$_6$H$_{11}$), 4.05 (dd, J = 4.2, 3.2 Hz, 1H, 5-*H*), 4.22 (s, 1H, 1-*H*), 4.55 (d, J = 14.6 Hz, 1H, NCH_2Ar), 4.70 (d, J = 14.6 Hz, 1H, NCH_2Ar), 7.24-7.37 (m, 5H, Ar-*H*).

(1*R*,2*S*,5*S*)-6-Benzyl-8-(cyclohexylmethyl)-6,8-diazabicyclo[3.2.2]nonan-2-ol (22a) and (1*R*,2*R*,5*S*)-6-Benzyl-8-(cyclohexylmethyl)-6,8-diazabicyclo[3.2.2]nonan-2-ol (23a)

21 (340 mg, 0.96 mmol) was dissolved in THF abs. (30 mL) and the mixture was cooled down to 0 °C. At this temperature, $LiAlH_4$ solution (1M in THF, 5.8 mL, 5.8 mmol) was added. The reaction mixture was stirred at 0 °C for 10 min and then

heated to reflux for 16 h. Finally H_2O was added under ice-cooling until H_2-liberation was finished. The mixture was stirred at 0 °C for 10 min and then heated to reflux for 30 min. After cooling to room temperature, the mixture was filtered and the solvent was removed in vacuo. The crude product was purified by fc (∅ 2 cm, h = 25 cm, v = 10 mL, C_6H_{12}/EtOAc = 9.5/0.5). $C_{21}H_{32}N_2O$, M_r = 328.5.

22a: (R_f = 0.30). Colorless oil, yield 69.4 mg (22%). ^{1}H NMR ($CDCl_3$): δ = 0.87-0.96 (m, 2H, $NCH_2C_6H_{11}$), 1.14-1.27 (m, 4H, $NCH_2C_6H_{11}$), 1.46-1.53 (m, 1H, $NCH_2C_6H_{11}$), 1.57-1.79 (m, 7H, $NCH_2C_6H_{11}$ (4H), 3-*H,* 4-*H*, O-*H*), 1.88-1.93 (m, 1H, 3-*H* or 4-*H*), 2.10 – 2.17 m, 1H, 3-*H* or 4-*H*), 2.25 (t, J = 10.4 Hz, 1H, $NCH_2C_6H_{11}$), 2.62-2.69 (m, 3H, $NCH_2C_6H_{11}$, NCH_2, 1-*H*), 2.72-2.92 (m, 4H, 5-*H*, NCH_2), 3.70 (s, broad, 2H, NCH_2Ar), 3.79-3.82 (m, 1H, 2-*H*), 7.21-7.34 (m, 5H, Ar-*H*).

23a: (R_f = 0.14). Colorless oil, yield 131.6 mg (42%). ^{1}H NMR ($CDCl_3$): δ = 0.81-0.92 (m, 2H, $NCH_2C_6H_{11}$), 1.17-1.26 (m, 3H, $NCH_2C_6H_{11}$), 1.33-1.43 (m, 1H, $NCH_2C_6H_{11}$), 1.64-1.85 (m, 9H, $NCH_2C_6H_{11}$ (5H), 3-*H,* 4-*H* (2H), O-*H*), 2.14-2.21 (m, 1H, 3-*H*), 2.31-2.40 (m, 2H, $NCH_2C_6H_{11}$), 2.72-2.80 (m, 4H, NCH_2, 1-*H*), 2.86-2.89 (m, 1H, 5-*H*), 3.11-3.14 (m, 1H, NCH_2), 3.72 (d, J = 13.3 Hz, 1H, NCH_2Ar), 3.77 (d, J = 13.4 Hz, 1H, NCH_2Ar), 4.02-4.06 (m, 1H, 2-*H*), 7.26-7.40 (m, 5H, Ar-*H*).

Receptor binding studies

The affinity towards σ_1 and σ_2 receptors was recorded as described in references 48-51 and 53.

Molecular Modeling

The optimized structure of selected compounds **14**, **15**, **22a**, and **23a** was docked into the σ_1-R putative binding pockets by applying a consolidated procedure.[38-40,57-61] All docking experiments were performed with *Autodock 4.2/Autodock Tools 1.4.6*[63]

on a win64 platform. The resulting docked conformations were clustered and visualized; then, for each compound, only the molecular conformation satisfying the combined criteria of having the lowest (i.e., more favorable) Autodock energy and belonging to a highly populated cluster was selected to carry for further modeling.

The ligand/σ_1-R complex obtained from the docking procedure was further refined in *Amber 14*[64] using the quenched molecular dynamics (QMD) method as previously described.[58,60,61] According to QMD, the best energy configuration of each complex resulting from this step was subsequently solvated by a cubic box of TIP3P [I] H_2O molecules extending at least 10 Å in each direction from the solute. The system was neutralized and the solution ionic strength was adjusted to the physiological value of 0.15 M by adding the required amounts of Na^+ and Cl^- ions. Each solvated system was relaxed by 500 steps of steepest descent followed by 500 other conjugate-gradient minimization steps and then gradually heated to a target temperature of 300 K in intervals of 50 ps of NVT MD, using a Verlet integration time step of 1.0 fs. The Langevin thermostat was used to control temperature, with a collision frequency of 2.0 ps^{-1}. The protein was restrained with a force constant of 2.0 kcal/(mol Å), and all simulations were carried out with periodic boundary conditions. Subsequently, the density of the system was equilibrated via MD runs in the isothermal−isobaric (NPT) ensemble, with isotropic position scaling and a pressure relaxation time of 1.0 ps, for 50 ps with a time step of 1 fs. All restraints on the protein atoms were then removed, and each system was further equilibrated using NPT MD runs at 300 K, with a pressure relaxation time of 2.0 ps. Three equilibration steps were performed, each 2 ns long and with a time step of 2.0 fs. To check the system stability, the fluctuations of the rmsd of the simulated position of the backbone atoms of the σ_1 receptor with respect to those of the initial protein were monitored. All physicochemical parameters

and rmsd values showed very low fluctuations at the end of the equilibration process, indicating that the systems reached a true equilibrium condition.

The equilibration phase was followed by a data production run consisting of 40 ns of MD simulations in the canonical (NVT) ensemble. Only the last 20 ns of each equilibrated MD trajectory were considered for statistical data collections. A total of 1000 trajectory snapshots were analyzed for each ligand/receptor complex.

The binding free energy, ΔG_{bind}, between the two ligands and the σ_1 receptor was estimated by resorting to the MM/PBSA approach implemented in *Amber 14*. According to this well-validated methodology.[38-40,57-61] the free energy was calculated for each molecular species (complex, receptor, and ligand), and the binding free energy was computed as the difference:

$$\Delta G_{bind} = G_{complex} - (G_{receptor} + G_{ligand}) = \Delta E_{MM} + \Delta G_{sol} - T\Delta S$$

in which ΔE_{MM} represents the molecular mechanics energy, ΔG_{sol} includes the solvation free energy and $T\Delta S$ is the conformational entropy upon ligand binding.

The *per residue* binding free energy decomposition was performed exploiting the MD trajectory of each given compound/σ_1-R complex, with the aim of identifying the key residues involved in the ligand-receptor interaction. This analysis was carried out using the MM/GBSA approach,[65,67] and was based on the same snapshots used in the binding free energy calculation.

All simulations were carried out using the *Pmemd* modules of *Amber 14*, running on our own CPU/GPU hybrid calculation cluster. The entire MD simulation and data analysis procedure was optimized by integrating *Amber 14* in modeFRONTIER, a multidisciplinary and multiobjective optimization and design environment.[68]

Supporting Information available

Supporting Information is available free of charge via the Internet at http://pubs.acs.org. and includes physical, spectroscopic and purity data of all compounds, synthetic methods and description of the σ receptor binding assays, cytotoxicity assay, induction of apoptosis and of the molecular modeling methods.

Corresponding author

Bernhard Wünsch*

Institute of Pharmaceutical and Medicinal Chemistry, University of Münster, Corrensstr. 48, D-48149 Münster, Germany

Tel.: +49-251-8333311; Fax: +49-251-8332144; E-mail: wuensch@uni-muenster.de

Acknowledgement

This work was supported by the *Deutsche Forschungsgemeinschaft (DFG)* which is gratefully acknowledged.

Abbreviations

APCI: atmospheric pressure chemical ionization; DTG: di-*o*-tolylguanidine; EM; exact mass; MM/PBSA: molecular mechanics/Poisson Boltzmann Surface Area; MTT: 3-(4,5-dimethylthiazol-2-yl)-2,5-diphenyltetrazolium bromide; PI: propidium iodide; SCLC: small cell lung cancer; SEM: standard error of the mean.

References

(1) Quirion, R.; Bowen, W. D.; Itzhak, Y.; Junien, L.; Musacchio, J. M.; Rothman, R. B.; Su, T. P.; Tam, S. W.; Taylor, D. P. A proposal for the classification of sigma binding sites. *Trends Pharmacol. Sci.* **1992**, *13*, 85–86.

(2) Hellewell, S. B.; Bruce, A.; Feinstein, G.; Orringer, J.; Williams, W.; Bowen, W.D. Rat liver and kidney contain high densities of σ_1 and σ_2 receptors, characterization by ligand binding and photoaffinity labeling. *Eur. J. Pharmacol*. **1994**, *268*, 9–18.

(3) Hanner, M.; Moebius, F. F.; Flandorfer, A.; Knaus, H. G.; Striessnig, J.; Kempner, E.; Glossmann, H. Purification, molecular cloning, and expression of the mammalian sigma1-binding site. *Proc. Natl. Acad. Sci. U. S. A.* **1996**, *93,* 8072–8077.

(4) Seth, P.; Fei, Y. J.; Li, H. W.; Huang, W.; Leibach, F. H.; Ganapathy, V. Cloning and functional characterization of a σ receptor from rat brain. *J. Neurochem.* **1998**, *70,* 922–931.

(5) Pan, Y. X.; Mei, J.; Xu, J.; Wan, B.-L.; Zuckerman, A.; Pasternak, G. W. Cloning and characterization of a mouse σ_1 receptor. *J. Neurochem.* **1998**, *70,* 2279–2285.

(6) Seth, P.; Leibach, F. H.; Ganapathy, V. Cloning and characterization of the type 1 sigma receptor from rat brain and structural analysis of the murine gene coding for the receptor. *The FASEB journal* **1998**, *12,* A161–A161.

(7) Kekuda, R.; Prasad, P. D.; Fei, Y. J.; Leibach, F. H.; Ganapathy, V. Cloning and functional expression of the human type 1 sigma receptor (hSigmaR1). *Biochem. Biophys. Res. Commun.* **1996**, *229,* 553–558.

(8) Moebius, F. F.; Reiter, R. J.; Hanner, M.; Glossmann, H. High affinity of sigma1-binding sites for sterol isomerization inhibitors: evidence for a pharmacological relationship with the yeast sterol C8-C7 isomerase. *Br. J. Pharmacol.* **1997**, *121,* 1–6.

(9) Ela, C.; Barg, J.; Vogel, Z.; Hasin, Y.; Eilam, Y. Sigma receptor ligands modulate contractility, Ca influx and beating rate in cultured cardiac myocytes. *J. Pharmacol. Exp. Ther.* **1994**, *269,* 1300–1309.

(10) Cobos, E. J.; Entrena, J. M.; Nieto, F. R.; Cendán, C. M.; DelPezo E. Pharmacology and therapeutic potential of sigma$_1$ receptor ligands. *Curr. Neuropharmacol*. **2008**, *6*, 344–366.

(11) Wolfe Jr., S. A.; Culp, S. G.; De Souza, E. B. σ-Receptors in endocrine organs: identification, characterization, and autoradiographic localization in rat pituitary, adrenal, testis, and ovary. *Endocrinology* **1989**, *124,* 1160–1172.

(12) Wolfe Jr., S. A.; Kulsakdinun, C.; Battaglia, G.; Jaffe, J. H.; De Souza, E. B. Initial identification and characterization of sigma receptors on human peripheral blood leukocytes. *J. Pharmacol. Exp. Ther.* **1988**, *247,* 1114–1119.

(13) Collier, T. L.; Waterhouse, R. N.; Kassiou, M. Imaging sigma receptors: applications in drug development. *Curr. Pharm. Des.*, **2007**, *13*, 51–72.

(14) Hayashi, T.; Su, T. P. Sigma-1 receptor chaperones at the ER-mitochondrion interface regulate Ca(2+) signaling and cell survival. *Cell* **2007**, *131,* 596–610.

(15) Brune, S.; Pricl, S.; Wünsch, B. Structure of the σ_1 receptor and Its ligand binding site. *J. Med. Chem.* **2013**, 56, 9809–9819.

(16) Johannessen, M.; Ramachandran, S.; Riemer, L.; Ramos-Serrano, A.; Ruoho, A. E.; Jackson, M. B. Voltage-gated sodium channel modulation by σ-receptors in cardiac myocytes and heterologous systems. *Am. J. physiol. Cell physiol.* **2009**, *296,* C1049–C1057.

(17) Zhang, H.; Cuevas, J. Sigma receptors inhibit high-voltage-activated calcium channels in rat sympathetic and parasympathetic neurons. *J. Neurophysiol.* **2002**, *87,* 2867–2879.

(18) Maurice, T.; Su T. P. The pharmacology of sigma-1 receptors. *Pharmacol. Ther.* **2009**, *124*, 195–206.

(19) Chien, C. C.; Pasternak, G. W. Selective antagonism of opioid analgesia by a sigma system. *J. Pharmacol. Exp. Ther.* **1994**, *271,* 1583–1590.

(20) Entrena, J. M.; Cobos, E. J.; Nieto, F. R.; Cendan, C. M.; Gris, G.; Del Pozo, E.; Zamanillo, D.; Baeyens, M. Sigma-1 receptors are essential for capsaicin induced mechanical hypersensitivity: studies with selective sigma-1 ligands and sigma-1 knockout mice. *Pain* **2009**, 143, 252−261.

(21) Wünsch, B. The σ1 receptor antagonist S1RA is a promising candidate for the treatment of neurogenic pain. *J. Med. Chem*. **2012**, 55, 8209−8210.

(22) Thomas G. E.; Szucs, M.; Mamone, J. Y.; Bem, W. T.; Rush, M. D.; Johnson, F. E.; Coscia, C. J. Sigma and opioid receptors in human brain tumors. *Life Science* **1990**, *46*, 1279–1286.

(23) Simony-Lafontaine, J.; Esslimani, M.; Bribes, E.; Gourgou, S.; Lequeux, N.; Lavail, R.; Grenier, J.; Kramar, A.; Casellas, P. Immunocytochemical

assessment of sigma-1 receptor and human sterol isomerase in breast cancer and their relationship with a series of prognostic factors. *Br. J. Cancer,* **2000**, *82*(12), 1958–1966.

(24) Wang, B.; Rouzier, R.; Albarracin, C. T.; Sahin, A.; Wagner, P.; Yang, Y.; Smith, T. L.; Meric-Bernstam, F.; Marcelo Aldaz, C.; Hortobagyi, G. N.; Pusztai, L. Expression of sigma 1 receptor in human breast cancer. *Breast Cancer Res. Treat.* **2004**, *87*(3), 205–214.

(25) Aydar, E.; Onganer, P.; Perrett, R.; Djamgoz, M. B.; Palmer, C. P., The expression and functional characterization of sigma (σ) 1 receptors in breast cancer cell lines. *Cancer Lett.* **2006**, *242*(2), 245–257.

(26) Vilner, B. J.; John, C. S.; Bowen, W. D. Sigma–1 and sigma–2 receptors are expressed in a wide variety of human and rodent tumor cell lines. *Cancer Res.* **1995**, *55*, 408–413.

(27) Spruce, B. A.; Campbell, L. A.; McTavish, N.; Cooper, M. A.; Appleyard, M. V.; O'Neill, M.; Howie, J.; Samson, J.; Watt, S.; Murray, K.; McLean, D.; Leslie, N. R.; Safrany, S. T.; Ferguson, M. J.; Peters, J. A.; Prescott, A. R.; Box, G.; Hayes, A.; Nutley, B.; Raynaud, F.; Downes, C. P.; Lambert, J. J.; Thompson, A. M.; Eccles, S. Small molecule antagonists of the sigma-1 receptor cause selective release of the death program in tumor and self-reliant cells and inhibit tumor growth in vitro and in vivo. *Cancer Res.* **2004**, *64*(14), 4875–4886.

(28) Colabufo, N. A.; Berardi, F.; Contino, M.; Niso, M.; Abate, C.; Perrone, R.; Tortorella, V. Antiproliferative and cytotoxic effects of some σ_2 agonists and σ_1 antagonists in tumor cell lines. *Naunyn Schmiedebergs Arch. Pharmacol.* **2004**, *370*, 106–113.

(29) Mach, R. H.; Smith, C. R.; Al–Nabulsi, I.; Whirrett, B. R.; Childers, S. R.; Wheeler, K. T. σ_2 Receptors as potential biomarkers of proliferation in breast cancer. *Cancer Res*. **1997**, *57*, 156–161.

(30) Platini, F.; Pérez–Tomas, R.; Ambrosio, S.; Tessitore, L. Understanding autophagy in cell death control. *Curr. Pharm. Des.* **2010**, *16*, 101–113.

(31) Crawford, K. W.; Bowen, W. D. Sigma–2 receptor agonists activate a novel apoptotic pathway and potentiate antineoplastic drugs in breast tumor cell lines. *Cancer Res*. **2002**, *62*, 313–322.

(32) Holl, R.; Schepmann, D.; Bednarski, P. J.; Grünert, R.; Wünsch, B. Relationships between the structure of 6–substituted 6,8–

diazabicyclo[3.2.2]nonan–2–ones and their sigma receptor affinity and cytotoxic activity. *Bioorg. Med. Chem*. **2009**, *17*, 1445-1455.

(33) Holl, R.; Schepmann, D.; Grünert, R.; Bednarski, P. J.; Wünsch B. Relationships between the structure of 6–allyl–6,8–diazabicyclo[3.2.2]nonane derivatives and their receptor affinity and cytotoxic activity. *Bioorg. Med. Chem*. **2009**, *17*, 777–793.

(34) Holl, R.; Schepmann, D.; Wünsch, B. Homologous piperazine–alcanols, chiral pool synthesis and pharmacological evaluation. *Med. Chem. Comm.* **2012**, *3*, 673–679.

(35) Azzariti, A.; Colabufo, N. A.; Berardi, F.; Porcelli, L.; Niso, M.; Simone, G. M.; Perrone, R.; Paradiso, A. Cyclohexylpiperazine derivative PB28, a sigma2 agonist and sigma1 antagonist receptor, inhibits cell growth, modulates p–glycoprotein, and synergizes with anthracyclines in breast cancer. *Mol. Cancer Ther*. **2006**, *5(7)*,1807–1816.

(36) Klebe, G. Drug Design: Methodology, concepts and mode-of-action, Springer, Heidelberg, **2013**.

(37) Geiger, C.; Zelenka, C.; Weigl, M.; Fröhlich, R.; Wibbeling, B.; Lehmkuhl, K.; Schepmann, D.; Grünert, R.; Bednarski, P. J.; Wünsch, B. Synthesis of bicyclic σ receptor ligands with cytotoxic activity. *J. Med. Chem.* **2007**, *50*, 6144–6153.

(38) Laurini, E.; Dal Col, V.; Mamolo, M. G.; Zampieri, D.; Posocco, P.; Fermeglia, M.; Vio, V.; Pricl, S. Homology Model and Docking-Based Virtual Screening for Ligands of the σ_1 Receptor. *ACS Med. Chem. Lett.* **2011**, *2*, 834–839.

(39) Brune, S.; Schepmann, D.; Klempnauer, K.–H.; Marson, D.; Dal Col, V.; Laurini, E.; Fermeglia, M.; Wünsch, B.; Pricl S. The sigma enigma: in vitro/in silico site-directed mutagenesis studies unveil σ_1 receptor ligand binding. *Biochem.* **2014**, *53*, 2993–3003.

(40) Weber, F.; Brune, S.; Korpis, K.; Bednarski, P. J.; Laurini, E.; Dal Col, V.; Pricl, S.; Schepmann, D.; Wünsch, B. Synthesis, Pharmacological evaluation, and σ_1 receptor interaction analysis of hydroxyethyl substituted piperazines. *J. Med. Chem*. **2014**, *57(7)*, 2884–2894.

(41) Lesma, G.; Colombo, A.; Sacchetti, A.; Silvani, A. metathesis based approach to diversely functionalized pyrrolizidines and indolizidines; total synthesis of (+)–monomorine. *J. Org. Chem*. **2009**, *74*, 590–596.

(42) Speicher, A.; Bomm, V.; Eicher, T. Dess–Martin–periodinan. *J. Prakt. Chem*. **1996**, *338*, 588–590.

(43) Joo, J. E.; Lee, K. E.; Pham, V. T.; Tian, Y. S.; Ham, W. H. Application of Pd(0)–catalyzed intramolecular oxazine formation of the efficient total synthesis of (–)–anisomycin. *Org. Lett.* **2007**, *18*, 3627–3630.

(44) Mentzel, M.; Hoffmann, H. M. R. N–Methoxy–N–methylamides (Weinreb amides) in modern organic synthesis. *J. Prakt. Chem*. **1997**, *339*, 517–524.

(45) Holl, R.; Dykstra, M.; Schneiders, M.; Fröhlich, R.; Kitamura, M.; Würthwein, E.-O.; Wünsch, B. Synthesis of 2,5–diazabicyclo[2.2.2]octanes by Dieckmann analogous cyclization. *Austr. J. Chem.* **2008**, *61*, 914–919.

(46) Bredt, J.; Thouet, H.; Schnitz, J. Über sterische Hinderung in Brückenringen (Bredtsche Regel) und über die *meso*–*trans*–Stellung in kondensierten Ringsystemen des Hexamethylens. *Liebigs Ann. Chem.* **1924**, *437*, 1–13.

(47) Warner, P. M. Strained bridgehead double bonds. *Chem. Rev.* **1989**, *89*, 1067–1093.

(48) Brune, S.; Schepmann, D.; Lehmkuhl, K.; Frehland, B.; Wünsch, B. Characterization of ligand binding to the σ(1) receptor in a human tumor cell line (RPMI 8226) and establishment of a competitive receptor binding assay. *Assay Drug Dev. Technol*. **2012**, *10*, 365–374.

(49) Meyer, C.; Neue, B.; Schepmann, D.; Yanagisawa, S.; Yamaguchi, J.; Würthwein, E.-U.; Itami, K.; Wünsch, B. Improvement of σ_1 receptor affinity by late-stage C-H-bond arylation of spirocyclic lactones. *Bioorg. Med. Chem*. **2013**, *21*, 1844–1856.

(50) Miyata, K.; Schepmann, D.; Wünsch, B. Synthesis and σ receptor affinity of regioisomeric spirocyclic furopyridines. *Eur. J. Med. Chem.* **2014**, *83*, 709–716.

(51) Hasebein, P.; Frehland, B.; Lehmkuhl, K.; Fröhlich, R.; Schepmann, D.; Wünsch, B. Synthesis and pharmacological evaluation of *like*- and *unlike*-configured tetrahydro-2-benzazepines with α-substituted benzyl moiety in 5-position. *Org. Biomol. Chem.* **2014**, *12*, 5407–5426.

(52) Bracht, K.; Boubakari; Grunert, R.; Bednarski, P. J. Correlations between the activities of 19 anti-tumor agents and the intracellular glutathione concentrations in a panel of 14 human cancer cell lines: comparisons with the National Cancer Institute data. *Anti-Cancer Drugs* **2006**, *17*, 41–51.

(53) Schepmann, D.; Lehmkuhl, K.; Brune, S.; Wünsch, B. Expression of sigma receptors of human urinary bladder tumor cells (RT–4 cells) and development of a competitive receptor binding assay for the determination of the affinity to human sigma2 receptors. *J. Pharm. Bio. Anal.* **2011**, *55*, 1136–1141.

(54) Korpis, K., Weber, F., Brune, S., Wünsch, B., Bednarski, P. J. Involvement of apoptosis and autophagy in the death of RPMI 8226 multiple myeloma cells by two enantiomeric sigma receptor ligands. *Bioorg. Med. Chem.* **2014**, *22*, 221–233.

(55) Skladanowski, A.; Konopa, J. Adriamycin and daunomycin induce programmed cell death (apoptosis) in tumour cells. *Biochem. Pharmacol*. **1993**, *46*, 375-382.

(56) Rebbaa, A.; Zheng, X.; Chou, P. M.; Mirkin, B. L. Caspase inhibition switches doxorubicin-induced apoptosis to senescence. *Oncogene* **2003**, *22*, 2805–2811.

(57) Laurini, E.; Marson, D.; Dal Col, V.; Fermeglia, M.; Mamolo, M. G.; Zampieri, D.; Vio, L.; Pricl, S. Another brick in the wall. Validation of the σ1 receptor 3D model by computer-assisted design, synthesis, and activity of new σ_1 ligands. *Mol. Pharm.* **2012**, *9*, 3107–3126.

(58) Meyer, C.; Schepmann, D.; Yanagisawa, S.; Yamaguchi, J.; Dal Col, V.; Laurini, E.; Itami, K.; Pricl, S.; Wünsch, B. Pd-catalyzed direct C-H bond functionalization of spirocyclic sigma-1 ligands: generation of a pharmacophore model and analysis of reverse binding mode by docking into a 3D homology model of the sigma-1 receptor. *J. Med. Chem.* **2012**, *55(18)*, 8047–8065.

(59) Rossi, D.; Pedrali, A.; Gaggeri, R.; Marra, A.; Pignataro, L.; Laurini, E.; Dal Col, V.; Fermeglia, M.; Pricl, S.; Schepmann, D.; Wünsch, B.; Peviani, M.; Curti, D.; Collina, S. Chemical, pharmacological, and in vitro metabolic stability studies on enantiomerically pure RC-33 compounds: promising neuroprotective agents acting as σ1 receptor agonists. *Chem. Med. Chem*. **2013**, *8(9)*, 1514–1527.

(60) Laurini, E.; Harel, D.; Marson, D.; Schepmann, D.; Schimdt, T. J.; Pricl, S.; Wünsch, B. Identification, pharmacological evaluation and binding mode analysis of novel chromene and chromane based σ_1 receptor ligands. *Eur. J. Med. Chem.* **2014**, *83*, 526–533.

(61) Zampieri, D.; Laurini, E.; Vio, L.; Fermeglia, M.; Pricl, S.; Wünsch, B.; Schepmann, D.; Mamolo, M. G. Improving selectivity preserving affinity: New piperidine-4-carboxamide derivatives as effective sigma-1-ligands. *Eur. J. Med. Chem.* **2015**, *90*, 797–808.

(62) Massova, I.; Kollman, P.A. Combined molecular mechanical and continuum solvent approach (MM-PBSA/GBSA) to predict ligand binding. *Perspect. Drug Discovery Des.* **2000**, *18*, 113–135.

(63) Morris, G. M.; Huey, R.; Lindstrom, W.; Sanner, M. F.; Belew, R. K.; Goodsell, D. S.; Olson, A. J. AutoDock4 and AutoDockTools4: automated docking with selective receptor flexibility. *J. Comput. Chem.* **2009**, *30*, 2785−2791.

(64) Case, D. A.; Berryman, J. T.; Betz, R. M.; Cerutti, D. S.; Cheatham, III, T. E.; Darden, T. A.; Duke, R. E.; Giese, T. J.; Gohlke, H.; Goetz, A. W.; Homeyer, N.; Izadi, S.; Janowski, P.; Kaus, J.; Kovalenko, A.; Lee, T. S.; LeGrand, S. Li, P. Luchko, T.; Luo, R.; Madej, B.; Merz, K. M.; Monard, G.; Needham, P.; Nguyen, H.; Nguyen, H. T.; Omelyan, I.; Onufriev, A.; Roe, D. R.; Roitberg, A.; Salomon-Ferrer, R.; Simmerling, C. L.; Smith, W.; Swails, J.; Walker, R. C.; Wang, J.; Wolf, R. M.; Wu, X.; York D. M.; Kollman P. A. (2015), *AMBER* **2015**, University of California, San Francisco.

(65) Jorgensen, W. L.; Chandrasekhar, J.; Madura, J. D.; Impey, R. W.; Klein, M. L. Comparison of simple potential functions for simulating liquid water. *J. Chem. Phys.* **1983**, *79*, 926−935.

(66) Tsui, V.; Case DA. Theory and applications of the generalized born solvation model in macromolecular simulations. *Biopolymers*, **2000**, *56*, 75−291.

(67) Onufriev, A.; Bashford, D.; Case, D.A. Modification of the generalized born model suitable for macromolecules. *J. Phys. Chem. B*, **2000**, *104*, 3712−3720.

(68) http://www.esteco.com/home/mode_frontier/mode_frontier.html.

Table of Contents Graphic